JOURNAL OF PETROLOGY | VOLUME 41 | NUMBER 5 | PAGES 605–625 | 2000

Episodic Silicic Volcanism in Patagonia and the Antarctic Peninsula: Chronology of Magmatism Associated with the Break-up of Gondwana

R. J. PANKHURST[1,2]*, T. R. RILEY[1], C. M. FANNING[3] AND S. P. KELLEY[4]

[1]BRITISH ANTARCTIC SURVEY, NATURAL ENVIRONMENT RESEARCH COUNCIL, HIGH CROSS, MADINGLEY ROAD, CAMBRIDGE CB3 0ET, UK

[2]NERC ISOTOPE GEOSCIENCES LABORATORY, KEYWORTH, NOTTINGHAM NG12 5GG, UK

[3]RESEARCH SCHOOL OF EARTH SCIENCES, THE AUSTRALIAN NATIONAL UNIVERSITY, CANBERRA, A.C.T. 0200, AUSTRALIA

[4]DEPARTMENT OF EARTH SCIENCES, THE OPEN UNIVERSITY, WALTON HALL, MILTON KEYNES MK7 6AA, UK

RECEIVED FEBRUARY 22, 1999; REVISED TYPESCRIPT ACCEPTED OCTOBER 5, 1999

New SHRIMP U–Pb zircon, Rb–Sr whole-rock, and ^{40}Ar–^{39}Ar data are presented for the Jurassic silicic volcanic rocks and related granitoids of Patagonia and the Antarctic Peninsula. U–Pb is the only reliable method for dating crystallization in these rocks; Rb–Sr is prone to hydrothermal resetting and Ar–Ar is additionally affected by initial excess ^{40}Ar. Volcanism spanned more than 30 My, but three episodes are defined on the basis of peak activity: V1 (188–178 Ma), V2 (172–162 Ma) and V3 (157–153 Ma). The first essentially coincides with the Karoo–Ferrar mafic magmatism of South Africa, Antarctica and Tasmania. The silicic products of V1 are lower-crustal melts that have incorporated upper-crustal material. The geochemistry of V2 and V3 ignimbrites is more characteristic of destructive plate margins, but the presence of inherited zircon still points to a crustal source. The pattern of volcanism corresponds in space and in time to migration away from the Karoo mantle plume towards the proto-Pacific margin of Gondwana during rifting and break-up. The heat required to initiate bulk crustal fusion may have been supplied by the spreading plume-head, but thinning of the crust during continental dispersion would also have facilitated anatexis.

KEY WORDS: *Antarctic Peninsula; ignimbrites; Jurassic; Patagonia; U–Pb; zircon*

INTRODUCTION

Jurassic magmatism in western Gondwana constituted the most voluminous episode of continental volcanism in the Phanerozoic era. During Early–Middle Jurassic time, some (2·5–3) × 10^6 km^3 of basalt and, to a lesser extent, rhyolite were erupted onto the supercontinent in its early stages of break-up. Recent high-precision geochronology (U–Pb and Ar–Ar) has shown that much of the basalt volcanism occurred during a very short period around 183–184 My ago (Encarnación *et al.*, 1996; Duncan *et al.*, 1997; Minor & Mukasa, 1997), but comparable studies of the silicic volcanism have so far been lacking. This paper is concerned with the chronology of the largest of these silicic outbursts, the Jurassic volcanic province of Patagonia and the Antarctic Peninsula. Although the emphasis here is on the geochronology and its significance for the history of volcanism, full geochemical and isotopic data will be presented in a companion paper (Riley *et al.*, 2000), which will also deal more completely with the petrogenesis of the rocks of this province.

General accounts of the Jurassic silicic volcanism of Patagonia have been given by Gust *et al.* (1985) and Pankhurst *et al.* (1998), the latter workers introducing the

*Corresponding author. Present address: NERC Isotope Geosciences Laboratory, Keyworth, Nottingham NG12 5GG, UK. Telephone: +44-115-936-3263. Fax: +44-0115-936-3302. e-mail: r.pankhurst@bas.ac.uk

all-encompassing term Chon Aike Province. Much of extra-Andean Patagonia is covered by undeformed rhyolitic ignimbrites, which are exposed in the structural highs of the North Patagonian and Deseado massifs (centred at latitudes of ~43°S and ~47°S, respectively; see Fig. 1). Borehole data show that these rocks extend beneath the intervening Cretaceous sedimentary basins. Andesites and basaltic andesites occur within the province, particularly in the west of the North Patagonian Massif, but are volumetrically less important. Similar Jurassic volcanic rocks, also largely rhyolitic in composition, occur in the southern Andes and in the Antarctic Peninsula; in both areas they are variably folded, tectonized and altered. Together, these volcanic rocks constitute one of the largest felsic magmatic fields known (~235 000 km^3, Pankhurst *et al.*, 1998). Until now, geochronological controls have not been sufficient to test either the assumed contemporaneity of the various volcanic groups within the province, or their precise relationship to Jurassic magmatism in other parts of southwestern Gondwana. Such tests are fundamental to assessing the significance of Jurassic magmatism in the rifting and subsequent break-up of the supercontinent, particularly with respect to any possible relationship to the Karoo mantle plume (see Storey *et al.*, 1992; Storey, 1995).

This paper presents and compares new data acquired by Rb–Sr, Ar–Ar and U–Pb zircon methods (including 21 ion microprobe ages), for samples from southern Patagonia and the Antarctic Peninsula; only the U–Pb method is considered fully reliable for these rocks. The results show that volcanism occurred over an extended period of time (*c.* 185–155 Ma), but was apparently concentrated in three discrete episodes (Early Jurassic, Middle Jurassic and Late Jurassic). The first of these is roughly coincident with the peak of Karoo–Ferrar basaltic volcanism.

STRATIGRAPHY AND PETROLOGY OF THE CHON AIKE PROVINCE AND RELATED ROCKS

The silicic volcanic outcrops of Patagonia and the Antarctic Peninsula are shown in Figs 1 and 2, respectively. In both regions the rocks have been subdivided into more localized formations or informal groups with individual characteristics [see Pankhurst *et al.* (1998) and Riley & Leat (1999) for reviews]. Brief summaries are given here.

The Marifil Formation (after Malvicini & Llambías, 1974) covers a large area in the northeast of Patagonia, mostly to the north of the Gastre fault zone (Rapela & Pankhurst, 1992). It largely consists of thick (25–100 m), flat-lying, strongly welded pink or red ignimbrite units and lesser rhyolite lava flows. Tuffs, lapilli-tuffs and volcanic agglomerates are interbedded with the ignimbrites, and the sequence is cut by sub-volcanic intrusions, including dacitic and andesitic dykes, which are considered to be co-magmatic with the ignimbrites (Rapela & Pankhurst, 1993).

The Chon Aike Formation (see Sruoga & Palma, 1984), up to 300 m thick, covers an area of some 100 000 km^2 in the Deseado Massif. Ignimbrites predominate, with subordinate epiclastic deposits, air-fall tuffs and intercalated lavas: the ignimbrites contain a wide variety of lithic clasts. The more highly welded examples are massive, with coarse columnar jointing; flattened *fiamme* occur but rheomorphic textures are rare. Some features suggest emplacement over wet sediments or subaqueously. The ignimbrites are phenocryst-poor rhyolites or leucocratic dacites. The principal minerals are quartz, K-feldspar, plagioclase and biotite, with accessory magnetite, ilmenite, apatite, zircon and monazite. The vitrophyres are characterized by perlitic texture; a variety of devitrification textures are displayed. Oxidation, silicification and hydrothermal alteration are widespread. The common alteration assemblage is quartz, sericite, calcite, albite and clay minerals.

The El Quemado, Ibañez and Tobífera formations of western Patagonia have been generally considered to be equivalent and consist of mainly silicic volcanic rocks that have been faulted, tilted and thrust as a result of Andean (Cretaceous–Tertiary) deformation. The Tobífera Formation is largely a sub-surface feature, revealed in boreholes in the Magallanes basin. The rocks of the El Quemado and Ibañez formations are similar to those of the Chon Aike Formation: rhyolitic ignimbrites associated with epiclastic sequences, air-fall tuffs, and breccias of various origins. They also contain some intercalated andesitic lava flows. The ignimbrites have a high content of lithic clasts and mineralogically a high content of plagioclase and Fe-rich biotite. In general, the degree of hydrothermal alteration, propylitic and chloritic, is significantly higher than in the Chon Aike Formation.

Thomson & Pankhurst (1983) assigned the majority of volcanic rocks in the Antarctic Peninsula to the Antarctic Peninsula Volcanic Group (APVG; Jurassic–Cenozoic), regarded as the long-term product of magmatic arc volcanism at the palaeo-Pacific margin. On the east coast of the northern Antarctic Peninsula (Graham Land), the Mesozoic sequences rest unconformably upon variably deformed quartzose metasedimentary rocks of the Trinity Peninsula Group (TPG; Permian–Triassic). In the southern Antarctic Peninsula (Palmer Land), they are associated with Middle to Late Jurassic sedimentary rocks.

The Mapple Formation (Riley & Leat, 1999), with a maximum observed thickness of ~1 km, represents the most widespread development of silicic volcanic rocks in the northern Antarctic Peninsula. Eruption was almost

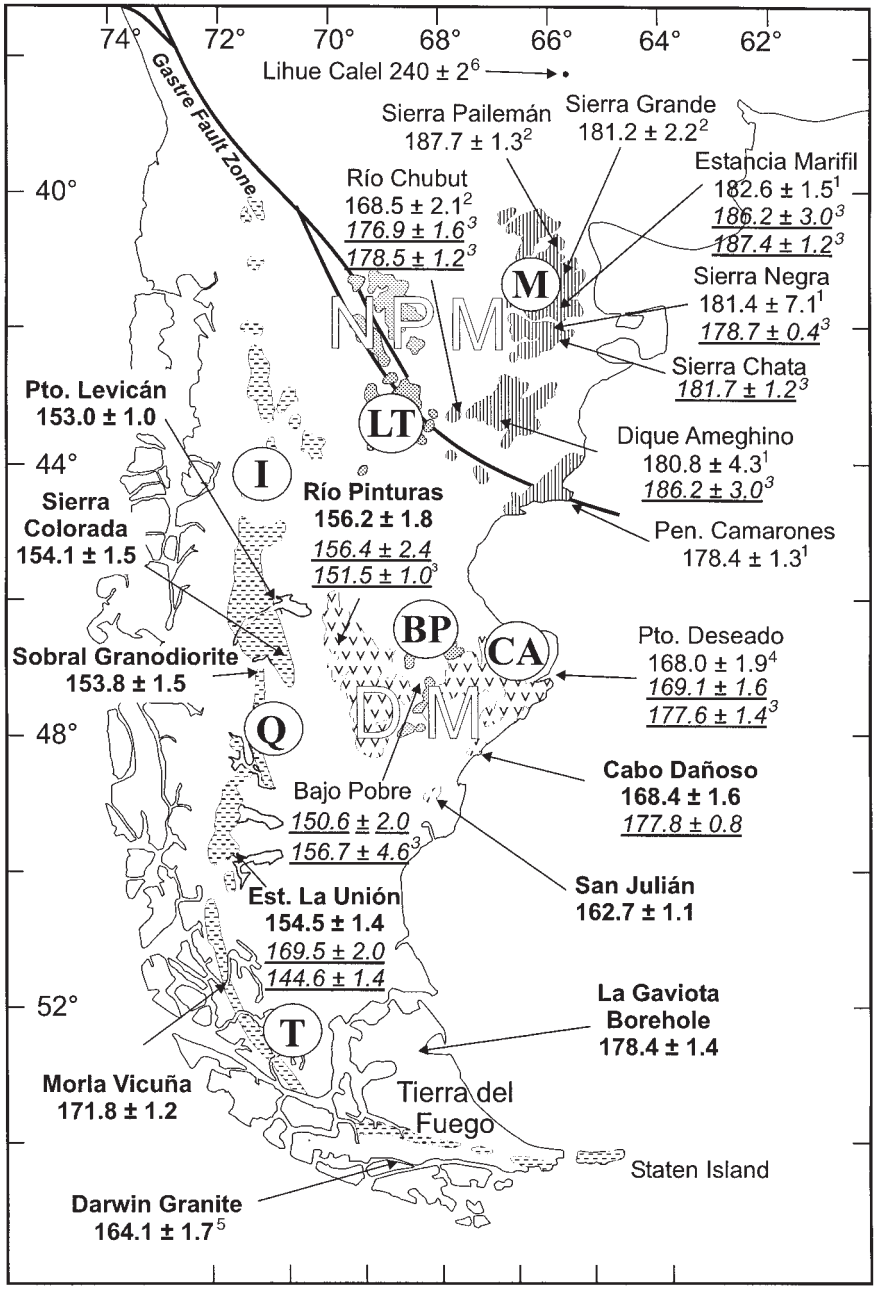

Fig. 1. Geochronological sketch map of Patagonia, showing the general outcrop patterns around the North Patagonian Massif (NPM) and the Deseado Massif (DM), and in the Andean Cordillera. Shading and letters in circles are used to distinguish the main volcanic formations: M, Marifil; CA, Chon Aike; Q, El Quemado; I, Ibañez; T, Tobífera; LT, Lonco Trapial (andesitic); BP, Bajo Pobre (basaltic–andesitic). High-precision geochronological data are also marked. Bold font, U–Pb; normal font, Rb–Sr; underlined font, Ar–Ar. Sources (superscript numbers): 1, Rapela & Pankhurst (1993); 2, Pankhurst & Rapela (1995); 3, Alric *et al.* (1996); 4, Pankhurst *et al.* (1993); 5, Mukasa & Dalziel (1996); 6, Rapela *et al.* (1996); otherwise new data from this paper. All ages are calculated to one significant decimal place for comparison and errors are given at the 2σ level.

entirely subaerial, and only locally subaqueous. Ignimbrite units (typically 5–20 m thick) predominate and, as in the Chon Aike Formation, exhibit wide variation in their degree of welding and lithic content. They are intercalated with minor air-fall units, lag breccias and lava flows. The Mapple Formation was metamorphosed up to greenschist facies and deformed, probably during the end-Jurassic Palmer Land compressional event (Kel-

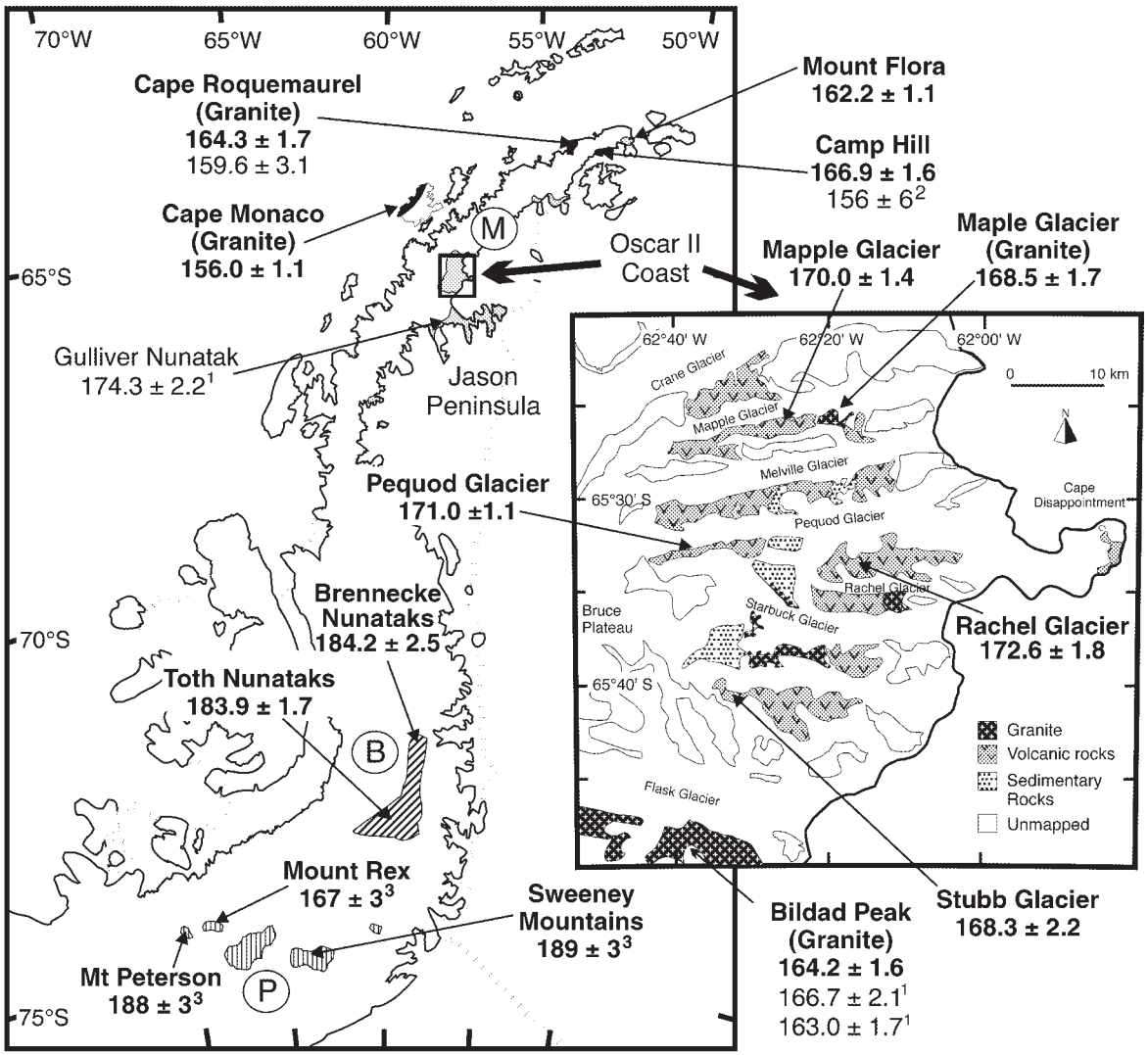

Fig. 2. Geochronological sketch map of the Antarctic Peninsula, showing the main outcrop areas of Jurassic volcanic rocks of the APVG and Jurassic granites (M, Mapple Formation; B, Brennecke Formation; P, Mount Poster Formation). High-precision geochronological data are also marked as in Fig. 1. Sources (superscript numbers): 1, Rb–Sr isochrons from Pankhurst (1982), calculated to one significant decimal place; 2, Sm–Nd isochron from Millar *et al.* (1990); 3, U–Pb results from Fanning & Laudon (1999); otherwise new data from this paper.

logg & Rowley, 1989). Steeply dipping cleavage is developed in epiclastic and many mudflow deposits, and increases in intensity westward. The ignimbrite units are poorly phyric, with an assemblage of embayed quartz, K-feldspar, plagioclase, biotite, magnetite, apatite, orthopyroxene, titanite, rutile and zircon. Feldspar is extensively replaced by calcite, sericite and clay minerals, and biotite is typically altered to chlorite. Spherulites in the rhyolitic ignimbrites indicate high-temperature devitrification.

The Brennecke Formation (Wever & Storey, 1992) comprises silicic metavolcanic units, cropping out at several localities in eastern Palmer Land (Fig. 2). At Brennecke Nunataks a sequence of massive dacitic to rhyolitic lava flows are interbedded with more foliated, welded pyroclastic rocks and black shales. A bimodal association has been recognized with an ~150 m thick succession of basaltic lavas (Hjort Formation; Wever & Storey, 1992).

The Mount Poster Formation (Rowley *et al.*, 1982) crops out in the southern Antarctic Peninsula and eastern Ellsworth Land (Fig. 2). It comprises dacitic to rhyodacitic pyroclastic rocks and lava flows, which reach a maximum total thickness of ~1–2 km. The succession is dominated by crystal-rich, grey or black welded ignimbrite units and minor lava flows. The ignimbrites contain abundant feldspar crystals; locally abundant lithic and pumice fragments confirm a pyroclastic origin. In the Sweeney

Mountains (Fig. 2), strongly welded ignimbrite units with oblate flattened pumice occur in association with rheomorphic ignimbrites, which have a well-defined parataxitic texture. The rhyolites contain abundant phenocrysts of plagioclase, sanidine, hornblende, embayed quartz and Fe–Ti oxides, with an alteration assemblage of sericite, clay minerals and calcite. The Mount Poster Formation is metamorphosed to chlorite grade (Rowley *et al.*, 1982).

PREVIOUS GEOCHRONOLOGY

Early attempts to date these rocks used the K–Ar whole-rock method, with highly variable results, compounded in most cases by a lack of good stratigraphical control. A comprehensive review by Cortés (1981) showed an age range of 240–125 Ma in Patagonia, albeit with a peak in the interval 165–155 Ma. From the northern Antarctic Peninsula, Rex (1976) determined three K–Ar ages of 190, 160 and 88 Ma. Subsequently, a single Rb–Sr isochron of 174 ± 2 Ma was published (Pankhurst, 1982), and an Sm–Nd isochron of 156 ± 6 Ma for garnets from a sill and volcanogenic sediments at the base of part of the succession (Millar *et al.*, 1990).

The first systematic dating in the Chon Aike province was by the Rb–Sr whole-rock method for the Marifil Formation (Rapela & Pankhurst, 1993). These data are shown in Fig. 1, together with other published and new high-precision results, all now calculated to one significant decimal place and with 2σ errors for comparability. Apart from any other conclusions, this shows that the Rb–Sr whole-rock technique in rhyolitic rocks is capable of precision equivalent to that of the other two methods. Rb–Sr isochrons for four localities yielded a tight range of 182·6 ± 1·5 to 178·4 ± 1·3 Ma, showing essential synchroneity in this area. Extension of the Rb–Sr method to the remainder of the Marifil Formation (Pankhurst & Rapela, 1995) slightly increased this range with further isochrons of 187·7 ± 1·3 Ma and 181·2 ± 2·2 Ma (the latter for two samples from a suite that was mostly reset at 174·1 ± 2·4 Ma). A significantly younger result of 168·5 ± 2·1 Ma was obtained for a suite from the Río Chubut section in the southwest of the outcrop area (Fig. 1); in this case, there was no evidence for resetting. However, the Ar–Ar results of Alric *et al.* (1996) from Río Chubut (176·9 ± 1·6 Ma and 178·5 ± 1·2 Ma, errors doubled from their originally quoted 1σ level) are within the range of the remaining Rb–Sr and Ar–Ar ages for the Marifil Formation (Fig. 1).

Pankhurst *et al.* (1993) obtained an Rb–Sr whole-rock age of 168·0 ± 1·9 Ma for samples of the Chon Aike Formation to the west of Puerto Deseado in southern Patagonia (Fig. 1), in agreement with a less precise result of 162 ± 11 Ma by the same method [De Barrio (1993), recalculated]. Alric *et al.* (1996) presented an Ar–Ar age of 177·6 ± 0·7 Ma from Puerto Deseado, significantly older than the Rb–Sr ages for the Chon Aike Formation.

In Tierra del Fuego, Mukasa & Dalziel (1996) determined a U–Pb zircon age (upper intercept) of 164·1 ± 1·7 Ma for a pluton in the peraluminous Darwin granite suite, thought to be correlative with the Tobífera Formation.

Subsequent to the Rb–Sr whole-rock isochron data of Pankhurst (1982), the only application of modern high-precision techniques in the Antarctic Peninsula is in the Mount Poster Formation (Fig. 2), where preliminary microprobe U–Pb zircon ages for rhyolites have been reported by Fanning & Laudon (1997, 1999) as 167 ± 3, 188 ± 3 and 189 ± 3 Ma. There is a clear need for new analytical work to resolve the discrepancies in the data for Patagonia and to amplify the data for the Antarctic Peninsula. The present study is an attempt to do this, and includes data both for the volcanic rocks and for a number of subvolcanic plutons inferred to be related to the volcanism.

ANALYTICAL METHODS

In this study we have relied chiefly on U–Pb zircon and Ar–Ar dating, methods that have the potential to yield meaningful information in rocks that might have suffered deformation, low-grade metamorphism and/or alteration. Samples were selected as far as possible to be representative of the various formations, with more intense sampling in the critical areas.

U–Pb dating was carried out using a sensitive high-resolution ion microprobe (SHRIMP II) at The Australian National University, Canberra, following the procedures of Compston *et al.* (1992). All zircon concentrates contained recognizable igneous crystals of a form associated with volcanism, e.g. 50–200 μm needles with aspect ratios of 3:1 to 10:1, simple prismatic terminations and often with hollow gas cavities along the centre of the grain. Many of the needles were broken, possibly as a result of explosive eruption of the ignimbrites. Cathodoluminescence examination showed regular zoning with no distinguishable cores or overgrowths. Analysis spots, mostly within the well-zoned ends of grains, were chosen to avoid cracks and inclusions. The final analytical data were treated as indicated below using Isoplot/Ex (Ludwig, 1999) and are presented in Table 1.

^{40}Ar–^{39}Ar dating was carried out by laser step-heating at The Open University, using procedures described by Kelley (1995). Most of the analysed material was hand-picked K-feldspar. Clear grains with feldspar cleavage were chosen from most samples. Occasionally, only milky grains could be found, indicating alteration; this was particularly so of the samples from the Andean outcrops

Table 1: Summary of SHRIMP U-Pb zircon results

Grain spot	U (ppm)	Th (ppm)	Age (Ma) $^{206}Pb/^{238}U$	SD	Grain spot	U (ppm)	Th (ppm)	Age (Ma) $^{206}Pb/^{238}U$	SD	Grain spot	U (ppm)	Th (ppm)	Age (Ma) $^{206}Pb/^{238}U$	SD
PAT.19.2 Cabo Dañoso					*PAT.62.2 Estancia La Unión*					*IBA-2 Puerto Levicán*				
1.1	104	55	167·4	3·5	1.1	340	156	151·3	2·6	1.1	382	178	150·3	1·9
2.1	181	111	164·9	2·8	1.2	304	130	153·4	2.9	2.1	464	196	155·5	1·9
3.1	382	275	174·5	2·4	2.1	330	145	150·7	2·3	3.1	499	230	151·7	1·8
4.1	250	143	166·5	4·8	3.1	449	304	153·1	2·0	4.1	586	342	155·3	1·8
5.1	243	175	167·5	3·0	4.1	202	86	151·2	3·8	5.1	576	348	154·5	1·9
6.1	155	125	176·5	4·6*	4.2	289	75	160·2	6.9	6.1	411	180	151·7	1·8
7.1	305	150	168·0	3·7	5.1	716	287	159·2	2·0	7.1	472	180	153·5	1·9
8.1	198	134	169·1	4·3	6.1	110	53	152·0	3·0	8.1	185	89	155·5	2·3
9.1	245	156	166·2	4·7	7.1	672	200	146·9	2·3	9.1	455	223	153·4	2·1
10.1	208	114	174·3	3·0	8.1	495	243	157·5	2·3	10.1	398	332	152·8	1·9
11.1	139	71	168·7	3·7	9.1	321	140	163·7	3·5	11.1	718	356	164·4	2·4*
12.1	460	247	168·4	1·9	10.1	264	106	154·4	2·7	12.1	330	157	152·9	2·1
13.1	216	130	165·3	2·4	11.1	516	414	156·4	2·5	13.1	376	213	153·3	1·9
14.1	161	114	170·1	5·3	11.2	659	575	152·6	3·2	14.1	598	369	150·0	1·9
15.1	156	83	170·7	4·3	12.1	244	108	155·2	3·0	15.1	252	173	151·9	2·0
16.1	77	45	167·9	3·4	13.1	166	64	154·8	2·3	Weighted mean			153·0	0·5
17.1	588	440	171·1	4·5	14.1	287	139	160·1	8·2					
Weighted mean			168·4	0·8	15.1	804	549	153·4	4·8					
					Weighted mean			154·5	0·7					
PAT.65.2 San Julián					*PAT.30.2 Río Pinturas*					*PAT.34.1 Sierra Colorada*				
1.1	356	224	169·0	4·6	1.1	199	114	156·8	2·8	1.1	579	267	155·7	1·9
1.1	384	186	161·7	2·0	2.1	282	208	153·9	4.1	2.1	294	154	154·5	2·2
7.1	636	458	155·2	1·8*	3.1	213	171	166·6	14·8	3.1	199	99	146·3	2·6*
8.1	479	204	161·0	2·1	3.2	160	117	155·6	4·7	4.1	321	292	153·4	2·1
13.1	667	258	161·3	1·8	4.1	545	203	159·1	2·2	5.1	225	152	152·5	2·3
12.1	306	124	160·6	2·1	5.1	423	284	158·5	3·2	6.1	1590	950	157·1	1·8
16.1	340	146	164·3	2·1	5.2	556	422	156·1	36·3	7.1	266	128	147·7	2·1*
17.1	249	164	160·4	1·9	6.1	403	200	151·5	2·8	8.1	278	127	155·9	2·6
18.1	263	120	164·5	2·1	7.1	244	192	155·9	2·7	9.1	442	132	151·4	2·1
19.1	435	288	171·4	9·3	8.1	269	111	306·4	6·2*	10.1	596	221	154·1	2·1
25.1	221	110	154·2	2·4*	9.1	263	213	158·7	5·5	11.1	681	404	155·7	2·0
26.1	322	139	162·2	2·0	10.1	245	125	161·9	4·6	12.1	300	77	157·0	2·3
27.1	203	125	162·5	5·7	11.1	62	46	147·5	4·6	13.1	321	162	151·4	2·2
30.1	251	133	164·4	2·4	11.2	154	150	150·2	2·2*	14.1	435	220	149·9	2·1
31.1	389	154	163·5	1·9	12.1	463	377	154·0	3·2	Weighted mean			154·1	0·6
32.1	163	92	161·2	2·4	13.1	586	560	161·2	3·9					
36.1	681	303	155·3	7·0	14.1	88	89	154·1	4·0					
39.1	161	72	163·9	2·3	15.1	173	162	153·0	26·3					
40.1	460	168	165·4	2·0	16.1	465	394	151·1	15·0					
Weighted mean			162·7	0·5	Weighted mean			156·2	0·9					

			Age (Ma)					Age (Ma)					Age (Ma)	
Grain spot	U (ppm)	Th (ppm)	$^{206}Pb/^{238}U$	SD	Grain spot	U (ppm)	Th (ppm)	$^{206}Pb/^{238}U$	SD	Grain spot	U (ppm)	Th (ppm)	$^{206}Pb/^{238}U$	SD
MV99-40 Canal Morla Vicuña					*R.4197.2 Toth Nunataks*					*R.6908.7 Mapple Glacier*				
1.1	139	88	288·8	4·8*	1.1	266	85	181·4	2·3	1.1	420	252	167·5	16·2
2.1	2965	2080	173·2	1·8	2.1	571	43	224·0	2·4*	2.1	637	186	167·9	2·0
3.1	636	68	489·4	5·4*	3.1	228	99	186·1	2·4	3.1	704	273	172·6	1·9
4.1	3435	2190	175·4	3·2	4.1	125	75	183·7	2·9	4.1	325	144	171·0	2·3
5.1	2145	1194	174·9	1·8	5.1	241	191	182·2	2·4	5.1	294	104	170·9	2·1
6.1	1686	588	170·5	1·9	6.1	142	74	186·3	2·5	6.1	834	483	170·9	1·9
7.1	2811	893	173·7	2·3	7.1	79	47	175·9	3·7	7.1	313	138	172·0	2·2
8.1	2007	1225	171·6	1·9	8.1	307	70	215·1	2·9*	8.1	1337	464	170·1	1·8
9.1	2426	876	169·2	1·8	9.1	78	53	186·2	3·1	9.1	594	309	167·6	1·9
10.1	435	171	1143·5	11·8*	10.1	119	64	179·1	3·0	10.1	299	122	174·8	2·1
11.1	2695	1398	171·9	1·8	11.1	156	33	180·1	2·6	11.1	395	186	173·2	2·0
12.1	2447	1251	169·7	1·8	12.1	126	49	187·8	3·0	12.1	713	210	167·0	2·0
13.1	2714	1968	171·0	1·8	13.1	395	55	184·1	2·2	13.1	184	51	170·2	2·4
Weighted mean			171·8	0·6	14.1	201	85	187·6	2·5	14.1	259	134	171·7	4·3
					15.1	120	57	185·3	2·7	15.1	192	106	179·6	3·7*
					16.1	136	58	186·5	2·4	16.1	438	182	168·6	2·2
					17.1	159	83	181·3	2·6	17.1	1832	956	165·4	1·8
					18·1	386	153	301·5	3·7*	Weighted mean			170·0	0·7
					Weighted mean			183·9	0·9					
PAT.70.8 La Gaviota borehole					*R.4182.10 Brennecke Nunataks*					*R.6914.6 Pequod Glacier*				
1.1	253	107	174·3	3·5	1.1	179	86	536·9	7·6*	1.1	297	121	172·2	2·1
2.1	230	101	173·1	2·4	2.1	398	105	184·7	2·3	2.1	353	113	169·4	2·0
3.1	300	134	175·9	2·5	3.1	416	65	179·0	2·1	3.1	237	123	176·7	4·2
4.1	371	234	178·2	2·3	4.1	204	100	183·5	2·8	4.1	493	187	172·5	2·0
5.1	443	246	178·4	2·4	5.1	75	54	186·2	3·5	5.1	759	350	169·7	1·9
6.1	1532	713	177·3	2·2	6.1	195	168	184·7	2·7	6.1	321	223	155·9	2·2*
7.1	295	164	177·7	2·6	7.1	729	208	172·4	2·8*	7.1	279	105	168·9	2·1
8.1	933	361	181·3	2·2	8.1	188	97	183·8	2·8	8.1	262	77	177·8	2·1*
9.1	443	172	179·1	2·8	9.1	538	428	188·4	2·2	9.1	405	151	171·4	1·9
10.1	173	82	179·3	3·1	10.1	293	145	186·4	2·7	10.1	285	107	170·1	2·2
11.1	575	195	178·9	2·7	11.1	1724	184	192·4	5·1	11.1	301	135	171·9	2·1
12.1	388	137	182·6	2·5	12.1	294	143	189·8	3·1	12.1	633	219	175·1	2·1
13.1	352	290	182·2	2·8	13.1	732	104	179·9	2·0	13.1	222	81	170·3	2·1
Weighted mean			178·4	0·7	Weighted mean			184·2	1·2	14.1	456	156	170·1	1·9
										15.1	312	145	168·8	2·2
										16.1	868	368	172·2	1·9
										17.1	301	136	169·3	2·1
										Weighted mean			171·0	0·5

Table 1: continued

Grain spot	U (ppm)	Th (ppm)	Age (Ma) $^{206}Pb/^{238}U$	SD	Grain spot	U (ppm)	Th (ppm)	Age (Ma) $^{206}Pb/^{238}U$	SD	Grain spot	U (ppm)	Th (ppm)	Age (Ma) $^{206}Pb/^{238}U$	SD
R.6632.10 Stubb Glacier					*R.601.9 Mount Flora*					*R.312.2 Bildad Peak granite*				
1.1	106	91	164·1	4·3	1.1	1787	1500	164·6	1·9	1.1	479	374	142·9	6·2*
2.1	154	100	165·8	2·3	2.1	874	490	159·2	1·8	2.1	92	44	184·9	6·0*
3.1	321	243	160·4	2·0*	3.1	492	323	160·2	2·0	3.1	1749	2390	167·0	1·8
4.1	169	82	162·4	2·2	4.1	2461	1548	161·7	2·4	4.1	364	210	159·6	2·2
5.1	137	85	162·6	6·1	4.2	1391	535	162·8	1·8	5.1	488	431	166·2	2·4
6.1	88	35	167·4	3·0	5.1	1920	899	164·6	1·8	6.1	512	255	164·8	2·6
7.1	346	225	164·8	2·1	6.1	2479	1403	165·6	1·7	7.1	310	203	160·4	2·6
8.1	134	127	170·7	4·1	7.1	179	121	156·6	2·3*	8.1	533	241	163·9	2·3
9.1	212	138	170·9	2·5	8.1	852	541	159·7	1·8	9.1	207	63	165·1	3·3
10.1	82	44	164·9	2·7	9.1	2360	993	159·7	1·7	10.1	345	225	165·6	3·0
11.1	182	78	175·5	2·5	10.1	2260	1270	163·6	1·7	11.1	543	255	162·3	2·0
12.1	302	153	179·6	2·4*	11.1	2064	1000	162·0	1·8	12.1	422	174	161·1	2·1
13.1	118	78	169·5	9·4	12.1	1164	798	160·1	1·8	13.1	285	138	164·6	2·7
5·2	137	104	172·5	6·1	13.1	1164	546	163·2	1·8	14.1	306	211	169·9	3·2
14.1	135	82	173·3	2·5	14.1	2664	1215	162·3	1·7	15.1	1643	1487	186·7	2·3*
15.1	155	83	170·6	2·4	15.1	1506	687	162·2	1·8	16.1	486	331	160·8	2·2
16.1	298	166	175·2	8·9	Weighted mean			162·2	0·6	17.1	401	300	169·7	2·5
17.1	92	66	174·6	2·6						18.1	253	168	162·9	3·0
18.1	84	61	170·0	3·3						19.1	138	95	166·0	2·9
19.1	149	105	163·3	2·6						20.1	263	176	168·6	3·1
Weighted mean			168·3	1·1						Weighted mean			164·2	0·8
R.6619.4 Rachel Glacier					*R.631.1 Camp Hill*					*R.6906.3 Mapple Glacier granite*				
1.1	309	225	156·5	3·9*	1.1	170	101	165·4	2·8	1.1	1304	622	169·2	4·5
2.1	182	110	161·0	7·6	2.1	209	73	167·2	2·6	2.1	531	208	166·1	4·5
3.1	257	164	170·2	2·3	2.2	139	82	159·1	2·9*	3.1	3521	1257	178·2	6·7
4.1	229	114	169·8	2·1	3.1	72	27	164·7	3·6	4.1	454	191	167·3	2·2
5.1	210	101	167·7	2·6	4.1	139	46	162·9	4·2	5.1	591	121	243·6	13·6*
6.1	187	173	164·8	5·0	5.1	451	344	163·0	2·7	6.1	324	177	167·7	2·3
7.1	272	102	473·0	7·8*	6.1	156	48	167·4	3·1	7.1	1125	713	165·9	3·6
8.1	87	33	180·5	3·3	7.1	416	237	167·8	2·5	8.1	1592	376	171·9	4·4
9.1	482	253	175·7	1·9	8.1	144	57	173·0	3·4	9.1	383	165	161·0	5·6
10.1	360	216	170·5	6·2	9.1	187	131	173·1	3·5	9.2	957	333	2152·9	44·5*
11.1	152	109	195·2	3·2*	10.1	153	87	170·0	3·5	10.1	3549	1323	170·2	3·0
12.1	220	178	167·1	10·2	11.1	89	75	279·5	4·8*	11.1	1216	289	176·4	4·1
13.1	95	73	168·6	3·3	12.1	89	37	165·8	3·8	12.1	1999	712	167·6	3·3
14.1	145	120	163·9	5·2	13.1	473	460	168·1	2·3	13.1	275	142	164·2	4·7
15.1	158	84	179·1	3·6	14.1	165	132	163·2	3·0	14.1	358	229	164·2	4·4
16.1	246	134	181·3	2·4*	15.1	333	254	164·3	3·6	15.1	1923	423	182·7	5·2*
17.1	172	108	172·8	3·4	Weighted mean			166·9	0·8	16.1	2808	972	166·5	8·6
18.1	149	135	170·2	2·4						17.1	1104	366	170·9	2·4
19.1	512	258	174·1	2·3						18.1	983	369	167·2	5·9
20.1	326	217	174·4	2·1						19.1	1024	258	168·6	4·1
21.1	172	126	173·8	3·7						Weighted mean			168·5	0·8
22.1	257	201	177·3	2·3										
23.1	208	177	167·6	3·5										
24.1	724	355	173·9	1·9										
Weighted mean			172·6	0·9										

Grain spot	U (ppm)	Th (ppm)	Age (Ma) $^{206}Pb/^{238}U$	SD	Grain spot	U (ppm)	Th (ppm)	Age (Ma) $^{206}Pb/^{238}U$	SD	Grain spot	U (ppm)	Th (ppm)	Age (Ma) $^{206}Pb/^{238}U$	SD
R.505.4 Cape Monaco granite					*BR.060.1 Cape Roquemaurel granite*					*PAT.49.1 Sobral granodiorite*				
1.1	254	217	154·7	3·8	1.1	217	127	163·1	3·2	1.1	634	703	150·4	4·9
2.1	152	133	158·0	3·0	2.1	528	151	223·0	3·4*	2.1	444	121	146·4	6·5
3.1	213	139	153·4	2·1	3.1	120	48	164·3	12·0	3.1	618	458	153·9	1·7
4.1	240	179	158·1	3·1	4.1	92	32	470·5	10·6*	4.1	249	94	147·4	3·1
5.1	185	113	151·7	2·3	4.2	5791	199	209·7	3·7*	5.1	634	500	153·5	2·7
6.1	619	414	158·3	1·8	4.3	502	82	162·5	2·8	6.1	148	48	161·0	2·6*
7.1	185	109	157·6	2·0	4.4	1582	55	255·4	2·7*	6.2	280	115	158·2	2·6
8.1	303	190	156·5	2·1	5.1	214	131	165·6	2·8	7.1	402	208	156·1	1·9
9.1	208	127	156·6	2·0	6.1	297	44	454·8	7·5*	8.1	218	81	151·2	3·1
10.1	242	152	161·8	2·6*	7.1	538	148	364·5	6·4*	9.1	396	236	154·2	2·7
11.1	806	719	157·3	1·7	8.1	277	95	595·0	9·5*	10.1	205	106	153·1	3·0
12.1	196	103	155·1	2·5	9.1	150	59	161·6	3·8	11.1	297	216	154·1	3·0
13.1	224	107	157·1	2·3	10.1	1042	177	560·8	6·5*	12.1	313	113	145·8	2·1*
15.1	227	145	155·6	2·2	11.1	3890	1915	164·4	1·8	13.1	36	11	153·5	3·7
16.1	178	128	179·0	15·2*	12.1	206	74	164·9	2·8	13.2	240	106	152·9	3·2
17.1	334	236	156·6	2·6	13.1	424	99	611·6	15·0*	14.1	1170	1263	156·3	3·3
18.1	160	110	154·6	2·3	14.1	281	146	163·9	2·5	15.1	247	106	151·3	5·5
19.1	136	81	152·3	2·3	15.1	868	407	165.6	2·0	16.1	225	107	162·4	6·8
Weighted mean			156·0	0·6	Weighted mean			164·3	0·9	Weighted mean			153·8	0·7

*Data point excluded from age calculation.

of Patagonia. One basaltic andesite from the Bajo Pobre Formation contained primary biotite, which was analysed in preference to altered plagioclase feldspar in the same sample. The data are available from the *Journal of Petrology* web site, at http://www.petrology.oupjournals.org.

Localities from which the U–Pb and ^{40}Ar–^{39}Ar data were obtained were also sampled for Rb–Sr whole-rock analysis at NIGL, Keyworth, UK, using the combined X-ray fluorescence and mass-spectrometry method employed by Rapela & Pankhurst (1993) and Pankhurst & Rapela (1995). This was less successful than in the previous work in the Marifil Formation, in that statistically valid isochrons were not obtained, probably because of the higher degree of alteration exhibited by the volcanic rocks of southwestern Patagonia and the Antarctic Peninsula. The data are available from the *Journal of Petrology* web site.

NEW RESULTS

Rb–Sr whole-rock

The new Rb–Sr data for the Chon Aike Formation did not yield any well-constrained age. Possible errorchrons are highly dependent on the combination and exclusion of individual points, and range from 160 to 180 Ma even for the restricted type locality area around Puerto Deseado. In contrast to the previous concordant isochron results for the Marifil Formation, these data clearly indicate inhomogeneous or disturbed isotope systems.

Although somewhat more consistent, the new Rb–Sr analyses of whole rocks from the Mapple Formation of the Antarctic Peninsula fail to define a precise isochron; the full dataset ($n = 53$) has a mean square weighted deviation (MSWD) of 30. If the scatter is accommodated by expanding errors by the square-root of MSWD, an 'age' of 159 $\pm$ 5 Ma results. There is clear visual evidence that the scatter within local sub-groups is less marked (Fig. 3a), but these also provide only errorchrons. Thus samples from station R.6908 in the Mapple Glacier give 153 $\pm$ 5 Ma (MSWD = 6·9) and 18 samples from the southeastern Stubb Glacier give 163 $\pm$ 7 Ma (MSWD = 4·4). Initial $^{87}Sr/^{86}Sr$ ratios for these errorchrons are in the range 0·7066–0·7076, comparable with previous values from the Marifil and Chon Aike formations.

Finally, a granitic pluton on the west coast of the Antarctic Peninsula around Cape Roquemaurel gave an

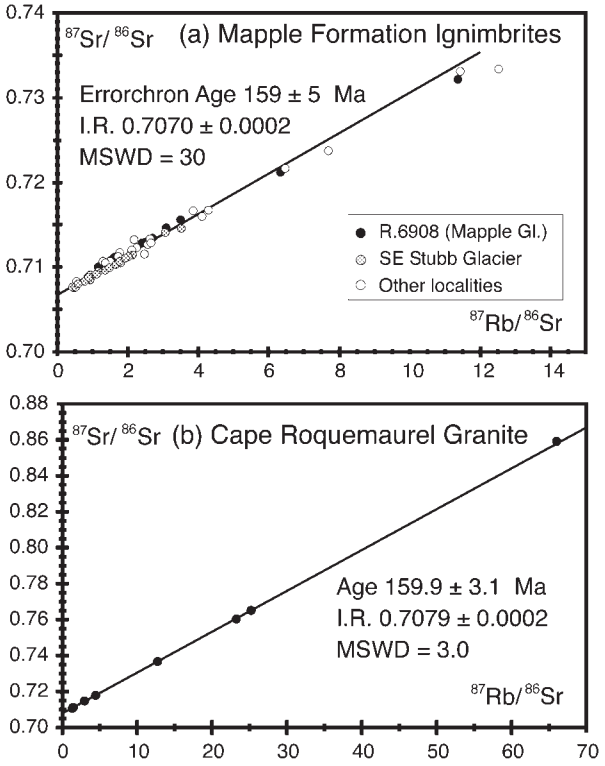

Fig. 3. Rb–Sr whole-rock isochron plots for (a) the Mapple Formation ignimbrites and (b) the Cape Roquemaurel granite, Antarctic Peninsula.

isochron age of 159·6 ± 3·1 Ma (Fig. 3b). A Jurassic age is thus established for this body. This contradicts previous estimates based on four K–Ar biotite ages averaging 141 ± 3 Ma [Rex (1976), recalculated to modern decay constants] and a conventional U–Pb zircon discordia, interpreted as indicating Palaeozoic inheritance combined with crystallization at 127 + 13/ − 25 Ma (Tangeman *et al.*, 1996).

U–Pb zircon

A total of nine samples from Patagonia and 12 samples from the Antarctic Peninsula were analysed. The U–Pb isotope data obtained, uncorrected for common Pb, are plotted in Tera–Wasserburg concordia diagrams in Figs 4–6. In these plots, concordant data should lie on a chord between the crystallization age and the coeval composition of common Pb, enabling us to distinguish points for zircons that contain older inheritance (displaced to the left of the main group) or that have suffered post-crystallization Pb loss (displaced to the right).

Clear examples of inherited grains are shown by ignimbrites from Canal Morla Vicuña (Tobífera Formation; 1144 and 490 Ma), Río Pinturas (?Chon Aike Formation; 306 Ma), Toth Nunataks (Brennecke Formation; 301, 224 and 215 Ma), Rachel Glacier (Mapple Formation; 473 and 195 Ma), and Camp Hill (Mapple Formation; 280 Ma). Similar inheritance is common in the Antarctic Peninsula granites: 186 and 185 Ma in the Bildad Peak granite, 244 and 183 Ma in the Mapple Glacier granite, and a variety of ages in the Cape Roquemaurel granite. The sample of the Mapple Glacier granite also contains one grain derived from a Neoproterozoic source (with a $^{207}Pb/^{206}Pb$ age of 2386 Ma). It must be emphasized that, as the focus of this work was on dating crystallization, these instances cannot be taken as representative of the age or degree of inheritance in the volcanic rocks. On the other hand, involvement of continental crust in the petrogenesis of the rhyolites is established by this inheritance. Obvious Pb loss is shown by one grain in the Pequod Glacier ignimbrite, Mapple Formation (156 Ma). Other rather more subjective cases of inheritance and/or Pb loss are shown by a number of samples; all excluded points are indicated in Table 1, which gives a summary of the SHRIMP ages: more complete data are available from the *Journal of Petrology* web site.

The inferred crystallization ages are calculated from the remaining concordant data in each case, as the weighted mean $^{238}U–^{206}Pb$ age after correction for common Pb, assessed using the $^{207}Pb/^{206}Pb$ ratio and model values according to Cumming & Richards (1975).

The U–Pb crystallization ages from Patagonia range from 154 to 168 Ma, but are individually precise. The oldest age, 178·4 ± 1·4 Ma, is for a sample of the Tobífera Formation from a depth of 2518 m in a borehole that hit basement at 4040 m. A second sample from this formation, from the western side of the Andes, gave a somewhat younger age of 171·8 ± 1·2 Ma. The Chon Aike Formation yielded ages of 168·4 ± 1·6 Ma from Cabo Dañoso and 162·7 ± 1·1 Ma from Bajo San Julián. Five samples from west of the Deseado massif (Fig. 1) give consistent ages of 153–156 Ma. One of these is an ignimbrite from the type locality of the El Quemado Formation at Estancia La Unión, and another from a caldera complex at Sierra Colorada. The latter had previously given an Rb–Sr whole-rock errorchron age of 136 ± 6 Ma (Pankhurst *et al.*, 1993); it is now clear that this cannot be the age of crystallization. A third sample in this age group is from the outcrop at Río Pinturas, which is generally attributed to the Chon Aike Formation, as the volcanic rocks here are flat-lying like those near the Atlantic coast. However, continuity of outcrops is not easily established, and it seems that at least some volcanism in the western Deseado Massif may have been synchronous with the El Quemado Formation. The youngest age of 153·0 ± 1·0 Ma is for a sample of the Ibañez Formation, which is generally considered as the Chilean equivalent of the El Quemado. The final sample in this age group is for the hornblende-phyric Sobral granodiorite of the Monte San Lorenzo massif (Ramos

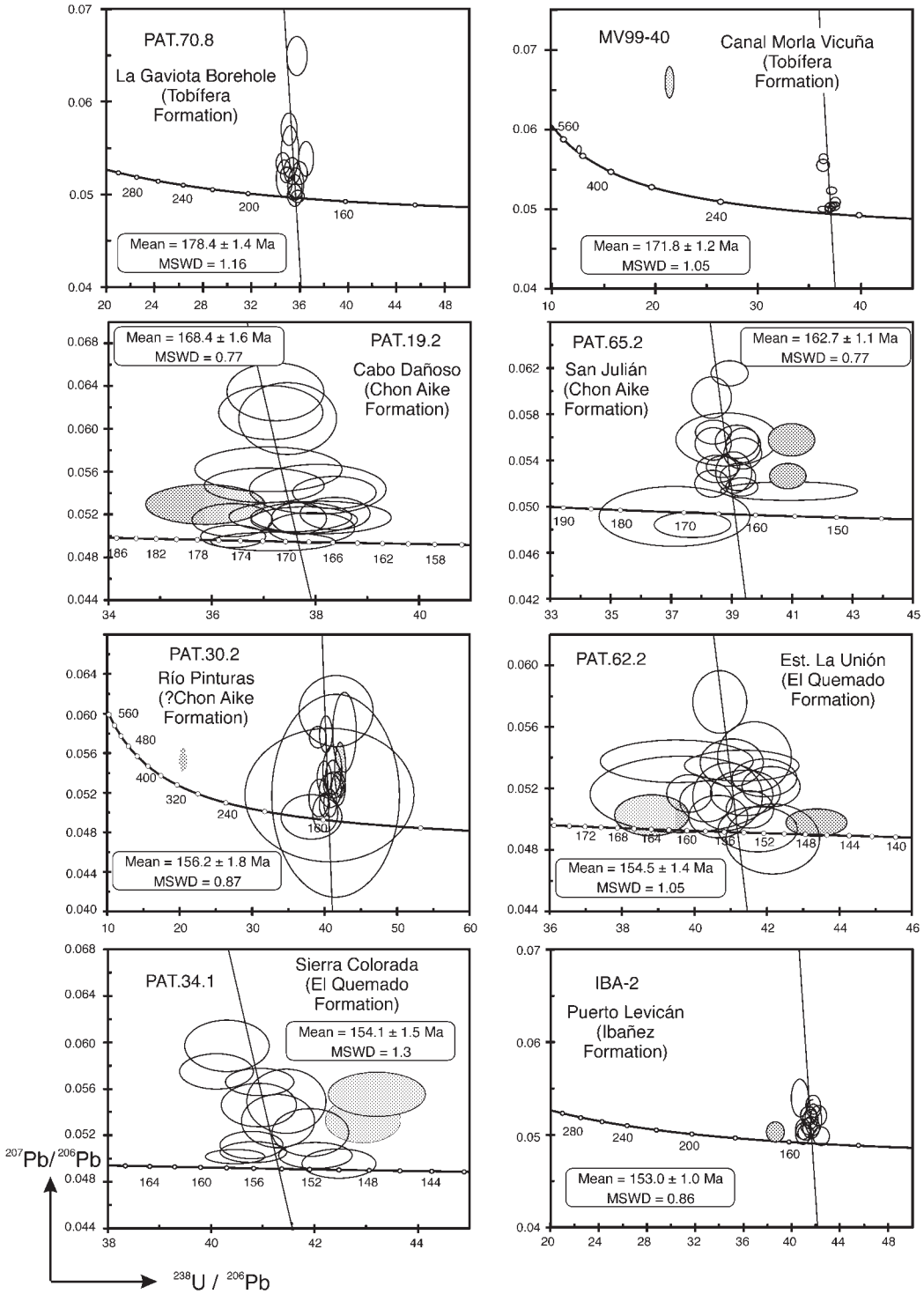

Fig. 4. U–Pb SHRIMP Tera–Wasserburg concordia plots for zircons from ignimbrites from Patagonia. Shaded points are excluded from age calculation. Localities shown in Fig. 1.

& Palma, 1981). This pluton was previously thought to be of Palaeozoic age but is now confirmed as penecontemporaneous (and cogenetic?) with the Jurassic volcanism of the Andes.

In the Antarctic Peninsula, two ignimbrite samples from the Brennecke Formation gave consistent ages of 184·2 ± 2·5 and 183·9 ± 1·7 Ma, comparable with the Rb–Sr ages of the Marifil Formation of Patagonia, with

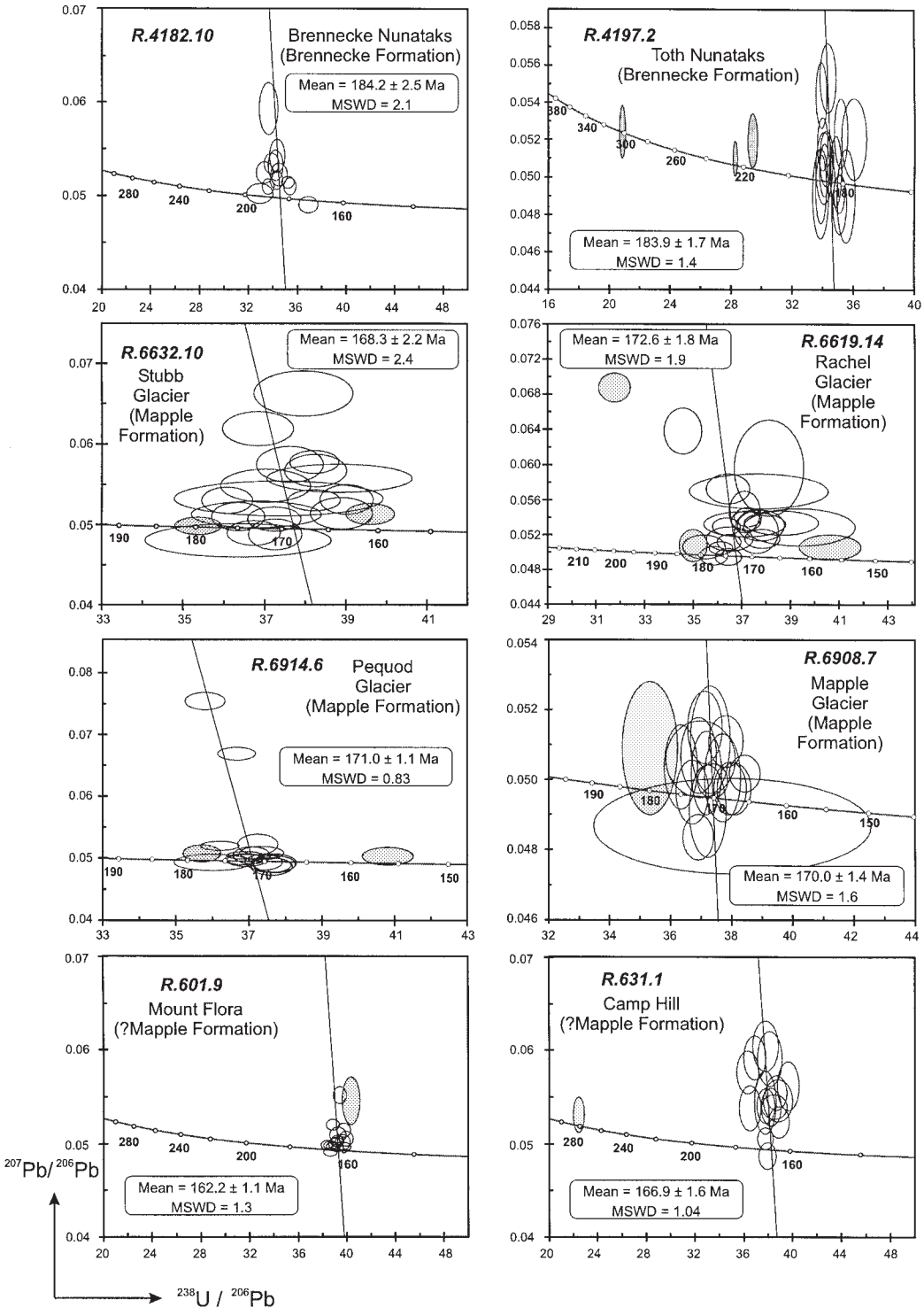

Fig. 5. U–Pb SHRIMP Tera–Wasserburg concordia plots for zircons from ignimbrites from the Antarctic Peninsula. Shaded points are excluded from age calculation. Localities shown in Fig. 2.

which it shares some geochemical features. As shown in Fig. 2, these are also similar to the older ages from the Mount Poster Formation at the southern end of the Antarctic Peninsula (Fanning & Laudon, 1997, 1999).

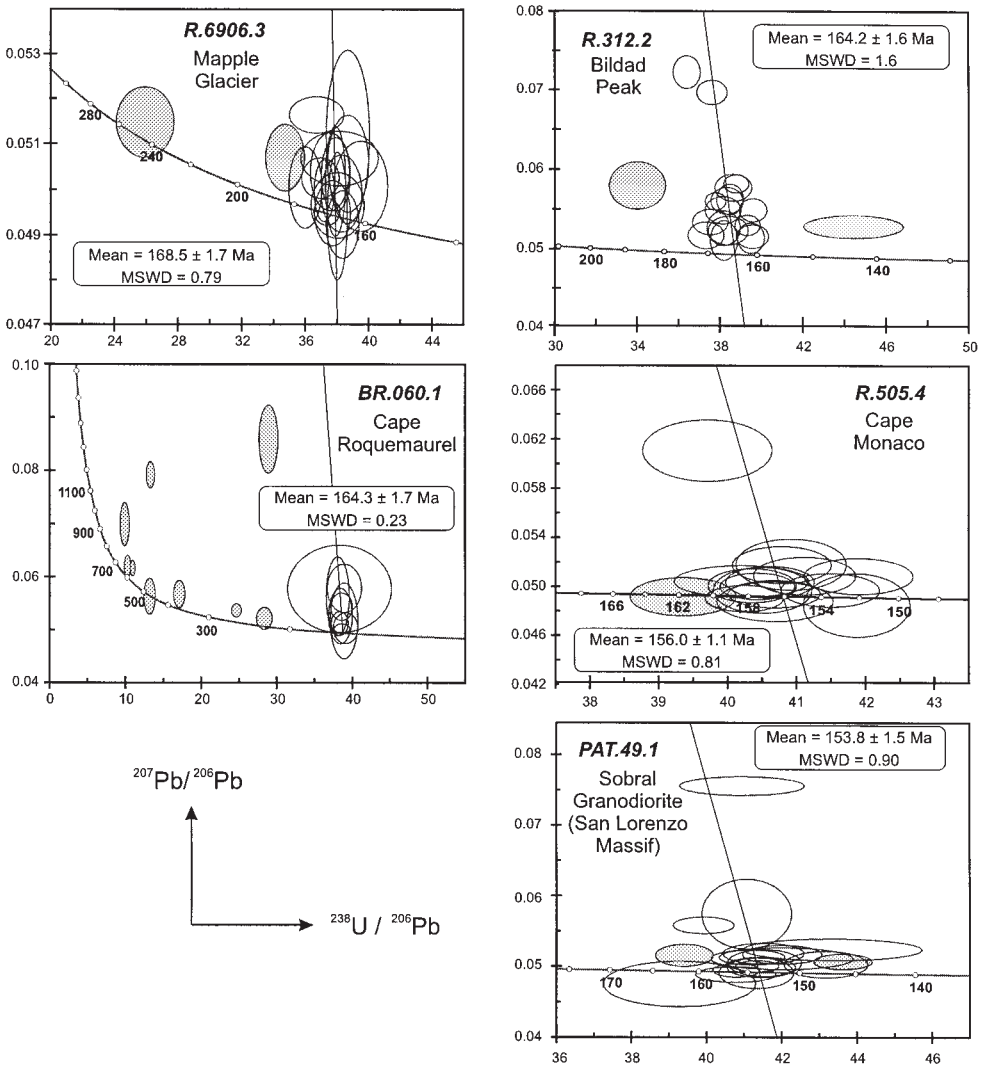

Fig. 6. U–Pb SHRIMP Tera–Wasserburg concordia plots for zircons from subvolcanic granite bodies from Patagonia and the Antarctic Peninsula. Shaded points are excluded from age calculation. Localities shown in Fig. 2.

However, the main group of new ignimbrite ages, from the Mapple Formation in the area around the Mapple Glacier (Fig. 2), fall in the range 168–173 Ma. The oldest of these is given by a sample from near the base of the sequence (R.6619.4, Rachel Glacier) and the youngest by a sample from near the top (R.6632.10, Stubb Glacier). Samples from the classic localities of Mount Flora and Camp Hill, where the volcanic rocks overlie sedimentary rocks of the Botany Bay Group, gave ages of 162·2 ± 1·1 and 166·9 ± 1·6 Ma, respectively. The granitic body intruded into the Mapple Formation ignimbrites, and considered to be magmatically associated with them (R.6906.3, Mapple Glacier), gave an age at the younger limit of this range. A similar granite from Bildad Peak gave an even younger age of 164·2 ± 2·0 Ma, which is concordant with Rb–Sr isochron ages of 166·7 ± 2·1 Ma and 163·0 ± 1·7 Ma previously obtained for this body (Pankhurst, 1982) and noted in Fig. 2. The Cape Roquemaurel granite gave an age of 164·3 ± 1·7 Ma, based on only nine measurements [this sample was primarily analysed for its inherited component, which is clearly more complex than the single upper intercept of the conventional U–Pb data reported by Tangeman *et al.* (1996)]. This age is concordant with that of the Bildad Peak granite and just within error of the Rb–Sr age reported above for Cape Roquemaurel. Finally, the Jurassic age of the Cape Monaco granite from the western side of the peninsula (156·0 ± 1·1 Ma) was unsuspected, but is consistent with continuation of plutonic activity following the end of the east coast volcanism. It is also

indistinguishable from the age of the Sobral granodiorite of the southern Andes.

Ar–Ar

Six samples were analysed, all from Patagonia (feldspar from five ignimbrites and biotite from one basaltic andesite). Ar–Ar temperature release patterns are shown in Fig. 7. Some of these seem relatively straightforward in that they show good medium- to high-temperature plateaux (five or more adjacent steps with the same age within experimental error). The result from Puerto Deseado (169·1 ± 1·6 Ma) appears reliable and is in agreement with the U–Pb result from Cabo Dañoso. The plateau for the latter locality itself (sample PAT.019.5) is more difficult to assess, as the large number of steps, resulting from overestimation of the necessary quantity of material, vary beyond expected error. The apparent age (177·8 ± 1·8 Ma) is significantly greater than the U–Pb age. It is possible that excess ^{40}Ar in fluid and solid inclusions was released during fracturing as a result of heterogeneous heating by the laser. Plateau ages were obtained from two samples from Estancia La Unión (169·5 ± 2·0 and 144·6 ± 1·4 Ma), but the calculated ages do not correspond to the U–Pb age of 154·5 ± 1·4 Ma for this locality, nor are they mutually consistent. In rapidly cooled volcanic rocks, the observed patterns of high initial ages, followed by a low and then climbing to a plateau, would normally be interpreted as gas release from altered material in the early few steps and from unaltered pure feldspar in the later steps. However, in the present case there is no correlation between the ages and ^{37}Ar/^{39}Ar (Ca/K) or ^{38}Ar/^{39}Ar (Cl/K) ratios, as might be expected if chemically altered material provided the gas released in the early steps. On the other hand, if subsolidus exsolution has taken place, these patterns may be more akin to the Ar-release patterns of plutonic K-feldspars or a mixture of K-feldspar and plagioclase, and the results might be interpreted as representing a cooling history, perhaps also affected by hydrothermally produced excess ^{40}Ar. The critical difference between interpreting a release pattern as a complex K-feldspar or a simple volcanic sanidine may be variation in chemistry with the progressive release. This is again true of the sample from Río Pinturas, which seems to show excess ^{40}Ar in the higher-temperature steps; the release shows a noisy increasing spectrum and no obvious variation in chemistry. The lower ages in the first half of the spectrum correspond more closely to the U–Pb age of 156·2 ± 1·8 Ma. Finally, data for the biotite separate from the Bajo Pobre basaltic andesite were treated by forcing an isochron fit though the composition of atmospheric Ar. With two points excluded, this yielded an age of 150·6 ± 2·0 Ma, within error of Alric *et al.*'s result of 156·7 ± 4·6 Ma for a sample from this formation.

DISCUSSION

Evaluation of the geochronological data

Rb–Sr data on these rocks have yielded statistically acceptable isochrons for only the very fresh ignimbrites of the Marifil Formation of northeast Patagonia and the granite plutons sampled from the Antarctic Peninsula. Concordance with published Ar–Ar ages (in the case of the former) and U–Pb data (for the latter) is taken as indicating that these Rb–Sr isochron ages are both reliable and equally precise. In all other cases, Rb–Sr data for the volcanic rocks scatter about rather crudely defined errorchrons. The scatter could be due either to initial heterogeneity in the volcanic magmas inherited from a heterogeneous source, or to post-crystallization disturbance. As the scatter is almost non-existent for the relatively fresh samples of the Marifil Formation and greatest for the obviously altered rocks of the Andean outcrops, we believe that the latter is the predominant cause. Some of the errorchrons give results that are concordant with the Ar–Ar or U–Pb ages, e.g. the previous Rb–Sr result of 168·0 ± 1·9 Ma for the Chon Aike Formation; although even here the errorchron is not substantiated by the new data obtained from the new sample collections. In general, the Rb–Sr errorchrons give apparent ages that are too young in comparison with the other methods. Their consistency at about 155–165 Ma for the well-sampled Mapple Formation suggests that they do, however, record a significant event, presumably the gradual closure of Rb–Sr systems to post-crystallization hydrothermal equilibration (Riley & Leat, 1999).

The U–Pb zircon data obtained in this study, which cover all main rock groups except the Marifil Formation of Patagonia, show a very consistent pattern of high-precision ages. In Patagonia, the two ages obtained from the Tobífera Formation are just outside error of each other and suggest an east–west younging from 178 to 172 Ma. Ages from the Chon Aike Formation in the eastern tracts of the Deseado Massif, and from the main volcanic outcrops of the northern Antarctic Peninsula, fall in the range 163–173 Ma, with a clear peak at 168–169 Ma. The 162 Ma age from Mount Flora, at the northern end of the Antarctic Peninsula, is slightly younger, but compares well with the age of the southernmost Chon Aike Formation sample at Bajo San Julián. Equivalence of the Chon Aike and Mapple formations seems very probable. The granites intruding the volcanic rocks of the Mapple Formation give ages of 169 Ma (Mapple Glacier) and 164 Ma (Bildad Peak), suggesting that emplacement was partially synchronous with the volcanism, but consistent with the field evidence that

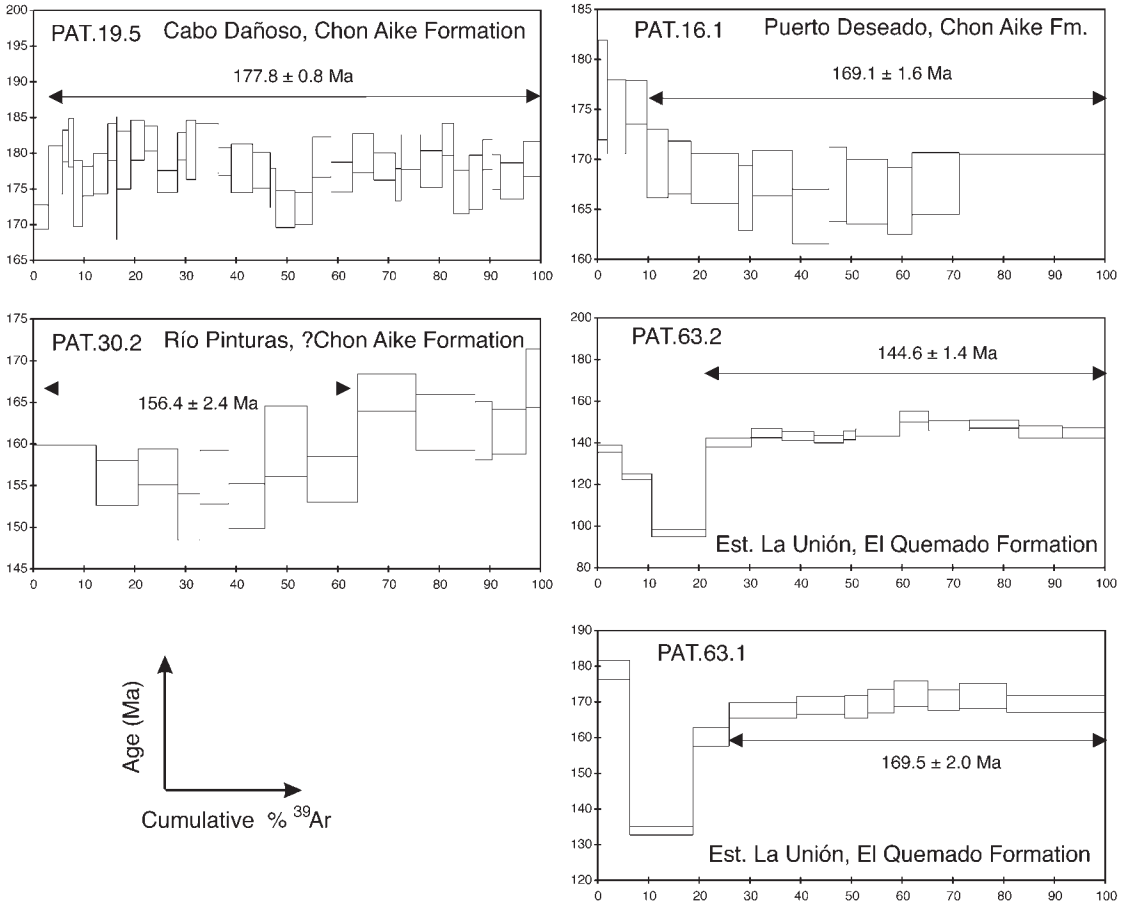

Fig. 7. Ar–Ar gas release spectra for feldspars from Patagonia. Localities shown in Fig. 1.

they are somewhat younger than the volcanic rocks. The oldest ages, obtained from the Brennecke Formation of the southern Antarctic Peninsula (184 Ma), are consistent with ages obtained for the Mount Poster Formation, which crops out even farther to the south (Fanning & Laudon, 1997, 1999). Contemporaneity of these southernmost ignimbrite outcrops with the Marifil Formation of Patagonia is established by comparison with the Rb–Sr and Ar–Ar ages of the latter. Outcrops of the ignimbrites in western Patagonia, including both the El Quemado Formation in the Andes and the westernmost outcrops of the Deseado Massif around Río Pinturas, yield significantly younger U–Pb ages of 155–156 Ma. This suggests that the Río Pinturas outcrops, although flat-lying and undeformed, should be considered correlative with the El Quemado Formation of the Andean region, rather than part of the Chon Aike Formation of the Deseado Massif. Small granite plutons, one in the Andes (San Lorenzo) and one on the west coast of the Antarctic Peninsula (Cape Monaco), have also given very similar ages of ~155 Ma, confirming their synchroneity, and probable genetic connection, with this later phase of silicic volcanism.

The new Ar–Ar ages obtained are in part concordant with the data of Alric *et al.* (1996) and in part with U–Pb, notably in the case of the Río Pinturas and Puerto Deseado samples (Fig. 1). There are, however, some notable discrepancies. The most worrying of these is the result of 177·8 ± 0·8 Ma for an ignimbrite from Cabo Dañoso, which is significantly older than the U–Pb age of 168·4 ± 1·6 Ma for the same locality. It is concordant with a similar Ar–Ar age of 177·6 ± 1·4 Ma from Puerto Deseado (Alric *et al.*, 1996), and also with the Rb–Sr isochron age of 178·4 ± 1·3 Ma from the southernmost outcrop of the Marifil Formation, at Península Camarones (Fig. 1). However, other Ar–Ar ages from the Chon Aike Formation are either within range of, or younger than, the U–Pb ages. We conclude that the samples that have yielded Ar–Ar feldspar ages older than U–Pb zircon ages for nearby volcanic rocks must contain excess ^{40}Ar, presumably incorporated during crystallization. The inconsistent Ar–Ar ages obtained from

Estancia La Unión, also mentioned above, are taken as evidence that the K–Ar isotopic system has been disturbed, involving redistribution of Ar in a manner not resolved by the Ar–Ar method. The Ar–Ar age of 150·6 ± 2·0 Ma for biotite from the Bajo Pobre Formation could suggest that this is broadly of the same age as the western Patagonian ignimbrites.

In conclusion, we believe that the most reliable geochronological results for the age of crystallization of the silicic rocks of the province are those given by the U–Pb zircon method. In certain cases, these results are supported by data from the Rb–Sr whole-rock and Ar–Ar methods (and extended geographically, as in the case of the Marifil Formation). In general, however, ages determined by the latter methods are subject to uncertainty related to hydrothermal effects or alteration.

The age pattern of volcanic activity

Figure 8 summarizes the data that we consider most reliable, as judged above, for the chronology of the silicic volcanic activity of Patagonia and the Antarctic Peninsula. Figure 9 illustrates the case for considering the activity to be episodic, with three principal phases identified. The Marifil Formation represents the initial burst of volcanism in the interval 178–188 Ma [mostly Toarcian according to the time-scale of Gradstein & Ogg (1996)]. At this stage, V1 could be considered a relatively long-lived episode, although it may be significant that no Marifil Formation rocks have yet been dated by the U–Pb method. The similar ages from the Mount Poster and Brennecke formations imply that a contemporaneous event is recorded in the southern Antarctic Peninsula. Interestingly, some of the subsequent Antarctic Peninsula granites show occasional evidence of zircon inheritance at ~185 Ma (Fig. 6), so that V1 volcanic rocks may be more widespread at depth than indicated by the present outcrop areas.

A second ignimbrite eruption event, V2, occurred throughout the eastern part of the Deseado Massif and along the eastern coast of the northern Antarctic Peninsula, at 162–172 Ma (with a marked peak at 168–170 Ma), including the Chon Aike and Mapple formations. In stratigraphical terms, this age corresponds to Bajocian–Bathonian, reasonably consistent with the best stratigraphical evidence. Stipanicic & Bonetti (1970) described a fossil flora of Callovian age from the volcanogenic sediments of the La Matilde Formation of Patagonia, which overlies and/or interdigitates with the Chon Aike Formation. A broader range of Middle–Upper Jurassic was ascribed to the flora by De Barrio *et al.* (1982). Eruption is usually considered to have occurred during the Upper Bajocian–Callovian interval (Di Giusto *et al.*, 1980). The ages obtained from Bajo San Julián and Mount Flora (162·7 ± 1·1 and 162·2 ± 1·1 Ma, respectively) would in fact be Callovian, so that a degree of local diachronism within the formation is implied.

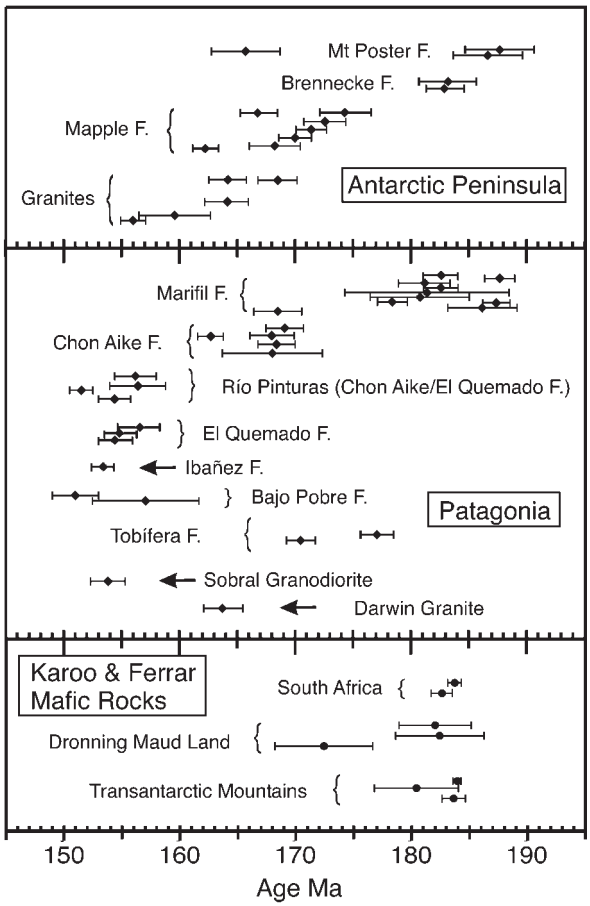

Fig. 8. Summary of the geochronology of the silicic volcanic rocks of Patagonia and the northern AP, together with associated granites. Only the most reliable age determinations of crystallization age have been plotted, consisting predominantly of the U–Pb zircon ages, the Rb–Sr whole-rock ages for the Marifil Formation and the granites, and Ar–Ar ages where these are concordant with those of either of the other methods.

Finally, we can identify a third event at 152–157 Ma (Oxfordian–Kimmeridgian), comprising the eastern Andean outcrops of ignimbrite and associated granite intrusions, and referred to here as V3. This includes both the El Quemado Formation and the supposedly correlative Ibañez Formation on the Chilean side of the Andes, for which K–Ar biotite ages in the range 152–135 Ma have been reported (Suárez & De La Cruz, 1997). At this stage we remain sceptical of the significance of previously reported Rb–Sr and K–Ar ages of less than 150 Ma for this group (e.g. Pankhurst *et al.*, 1993), as the clear evidence of this paper is that such ages are prone to resetting, probably by hydrothermal activity. On the basis of the limited Ar–Ar data, it is possible that

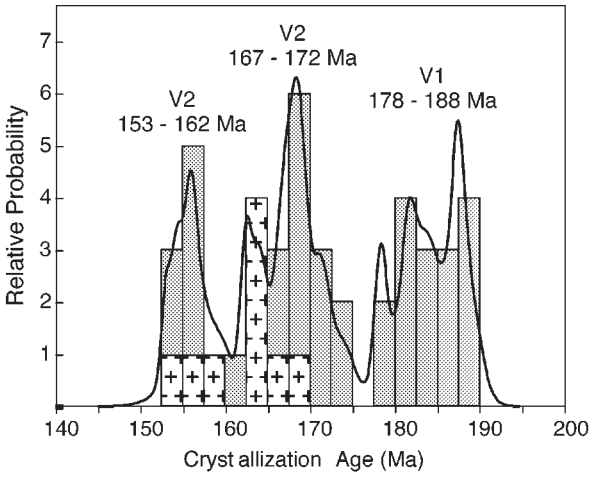

Fig. 9. Histograms and cumulative probability curve for the rhyolite and subvolcanic granite ages of Fig. 8, plotted using Isoplot/Ex (Ludwig, 1999). The plot indicates the three main volcanic events distinguished in this paper.

the Bajo Pobre Formation of basaltic andesites belongs to the V3 episode.

Two results obtained from the Tobífera Formation are slightly discrepant, perhaps indicating diachronism within this unit. The one from the borehole sample, farther east, gave an age at the younger limit of V1, whereas the other gave an age within the main interval of V2.

These data also establish the migration trends within the silicic province as a whole, as illustrated in Fig. 10. The earliest activity occurred in northeast Patagonia and the southern Antarctic Peninsula. During the V2 event, the locus of activity moved westwards in the Deseado Massif and northwards in the Antarctic Peninsula. The final volcanic–plutonic episode marked a clear westward migration of activity toward the proto-Pacific margin, both in Patagonia and in the Antarctic Peninsula. In the reconstruction shown, representing a possible configuration during V1, these trends constitute a continuous migration towards the Pacific margin. The final ignimbrite event appears to merge in time with the earliest plutonism of the Patagonian batholith, perhaps without any significant overlap (U–Pb zircon ages of ~150 Ma, Bruce *et al.*, 1991; Parada *et al.*, 1997). The main phase of Early Cretaceous growth in the Antarctic Peninsula batholith began ~142 My ago (Leat *et al.*, 1995).

Relationship to Jurassic magmatism elsewhere in Gondwana

As shown in Fig. 8, the age of V1 is essentially coincident with the major episode of pre-Gondwana break-up mafic magmatism represented in Antarctica (the Ferrar Supergroup of the Transantarctic Mountains and the Dronning Maud Land mafic igneous province), Australia (Tasmanian dolerites) and South Africa (Karoo province). High-precision geochronological data are available for all three phases of the Ferrar Supergroup: the Ferrar Dolerite (hypabyssal), the Kirkpatrick Basalt (volcanic) and the Dufek gabbro (plutonic). The Ferrar Dolerite has been dated using U–Pb zircon and baddeleyite at 183·6 ± 1·0 Ma (Encarnación *et al.*, 1996), and at 176·7 ± 3·6 Ma (Ar–Ar; Fleming *et al.*, 1997), although the latter age would be 180·2 Ma using the calibration standard of Renne *et al.* (1998). Ar–Ar ages of the Kirkpatrick Basalt suggest an age of 176·6 ± 3·6 Ma (Heimann *et al.*, 1994), but may be similarly recalculated to 180·5 ± 3·6 Ma. The age of emplacement of the Dufek Intrusion, the third component of the Ferrar Supergroup, has been determined as 182·7 ± 0·4 to 183·9 ± 0·3 Ma (U–Pb zircon; Minor & Mukasa, 1997) and 182·5 ± 4·8 Ma (Ar–Ar; Brewer *et al.*, 1996). [It should be noted that all previously published Ar–Ar ages referred to in this paper specified errors at the 1σ level; these have been doubled to compare with the standard 2σ errors on the U–Pb and Rb–Sr ages.]

The Jurassic magmatism of Dronning Maud Land, East Antarctica, has yielded two Ar–Ar ages (Brewer *et al.*, 1996) of 182·4 ± 3·8 Ma (dolerite sill) and 172·4 ± 4·2 Ma (basalt lava), whereas dolerite sills from the Theron Mountains farther south gave a range essentially between these two limits. The older age has been confirmed by Duncan *et al.* (1997), who carried out an Ar–Ar study on Kirwan basalts from Dronning Maud Land, which provided plateau ages of 181–183 Ma. Available age data for the mafic rocks of Tasmania and southeast Australia are restricted to K–Ar whole-rock ages, which give a range of 170–190 Ma (Hergt *et al.*, 1991).

A detailed study of both mafic and silicic volcanic rocks from the Karoo province indicates a total age range of 179–184 Ma (Ar–Ar; Duncan *et al.*, 1997), with a magmatic peak at 183 Ma. A new age for the Karoo dolerites of 183·7 ± 0·6 Ma (U–Pb zircon and baddeleyite; Encarnación *et al.*, 1996) confirms a very close temporal association between Ferrar and Karoo rocks, with a very short-lived episode of basic magmatism and intrusive activity (no more than 3 My). This may be seen as consistent with the Karoo mantle plume hypothesis (Brewer *et al.*, 1992; Cox, 1992).

The close correspondence in eruptive age between the V1 rhyolites of Patagonia and the Antarctica Peninsula on the one hand and the Karoo plume rocks on the other is emphasized by their relative geographical locations. In Fig. 9 it is clear that these Early Jurassic volcanic rocks were all erupted in a position close to the supposed position of the plume-head, whereas the subsequent V2 and V3 volcanic rocks represent migration away from the plume towards the palaeo-Pacific margin of Gondwana. This pattern clearly reflects the kinematics of

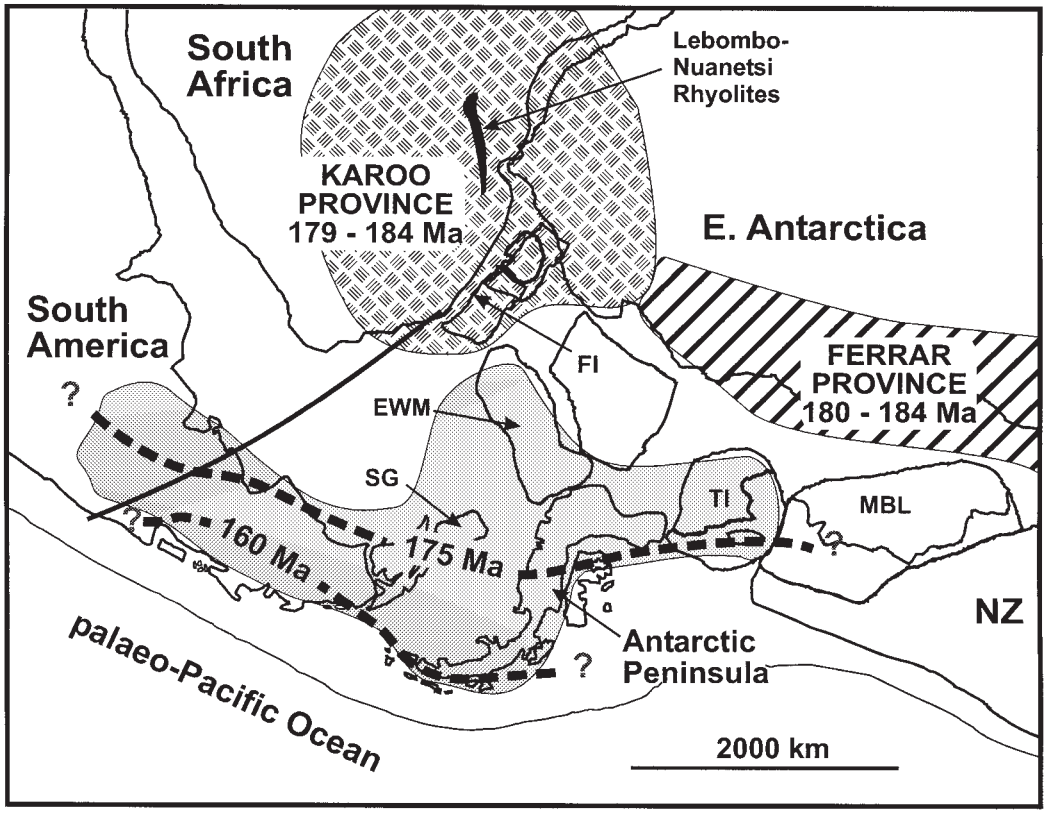

Fig. 10. Location and timing of the silicic volcanic province of Patagonia and the Antarctic Peninsula in relation to the Jurassic mafic magmatism of Gondwana. The base map is the early Jurassic reconstruction of Storey *et al.* (1992). The contours of 175 Ma and 160 Ma are drawn to separate the three silicic volcanic episodes identified in this paper. The first is essentially coincident with and adjacent to the Karoo and Ferrar mafic outcrops. The subsequent silicic episodes show migration towards the margin of the supercontinent during the period in which the smaller plates formed during break-up were dispersing. Crustal blocks: EWM, Ellsworth–Whitmore mountains; SG, South Georgia; FI, Falkland Islands; TI, Thurston Island; MBL, Marie Byrd Land.

break-up and dispersal of the smaller plates resulting from it.

The silicic volcanic rocks in the Lebombo–Nuanetsi region in the eastern part of the Karoo province, which are thought to have been generated by crustal melting over a lithospheric thin spot produced by the plume, show many similarities to the silicic rocks of the Marifil and Brennecke formations. These latter formations are older than the active margin rocks of South America and the Antarctic Peninsula, with a peak in eruptive age at *c.* 180–183 Ma that coincides precisely with the major Karoo mafic volcanic event. The V1 rhyolites exhibit a 'within-plate' geochemical signature, e.g. a tendency to high Nb and Zr contents. Their negative ε_{Nd} values of -4 to -9 (Wever & Storey, 1992; Pankhurst & Rapela, 1995; Pankhurst *et al.*, 1998) indicate a high level of continental crust involvement. Wever & Storey (1992) interpreted the Brennecke Formation as partly generated by crustal melting in an ensialic back-arc setting during lithospheric attenuation, possibly over a rising mantle diapir. For the Marifil Formation magmas, Pankhurst & Rapela (1995) used isotopic and geochemical modelling to deduce a lower-crustal granulitic source of Proterozoic age. Further geochemical data for the Mount Poster Formation (Riley *et al.*, 2000) indicate a variable degree of upper-crustal contamination for these rocks.

The silicic volcanic rocks erupted in Patagonia and the Antarctic Peninsula during the V2 and V3 events (Fig. 8) have no obvious counterparts in the plume-related mafic igneous activity of Gondwana, except that part of the Dronning Maud Land basalt sequence may be as young as the V2 event (Brewer *et al.*, 1996). These ignimbritic rocks generally have rather low Nb contents (<20 ppm), and little large ion lithophile element enrichment (Pankhurst *et al.*, 1998). They also have only slightly negative ε_{Nd_t} values in the range *c.* -2 to -5 (R. J. Pankhurst & T. R. Riley, unpublished data, 1999). Thus they are geochemically more typical of subduction-related rhyolites, although zircon inheritance, as well as the isotopic and geochemical data, still suggest a primary origin by anatexis of the continental crust [see further arguments given by Riley *et al.* (2000)]. In time and

space, their eruption coincides with a significant shift in the locus of volcanism towards the active Andean margin. In particular, the age of V3 (157–153 Ma) merges into the range of the initial plutonic emplacement of the Patagonian batholith, a coast-parallel feature clearly related to subduction of the Pacific ocean-floor beneath the South American continent.

The possible relationship of this volcanic history to earlier events in Patagonia is not clear at this stage. Unpublished data cited by Rapela *et al.* (1996) record an Early Triassic ignimbrite at Lihue Calel (Fig. 1). The succession here has given a Rb–Sr whole-rock isochron of 240 $\pm$ 2 Ma, Zr contents of up to 700 ppm and ε_{Nd_t} values of $-5{\cdot}4$ and $-8{\cdot}3$. A Late Triassic Rb–Sr age of 222 $\pm$ 2 Ma at Los Menucos, within the North Patagonian Massif, was supported by the associated occurrence of *Dichroidium*-bearing sedimentary rocks. The latter ignimbrites have ε_{Nd_t} values of -8 to $-9{\cdot}5$. These Triassic within-plate rhyolites are thus geochemically comparable with the V1 episode, but their eruption predates the Karoo plume by 40–60 My.

CONCLUSIONS

The high-precision age determinations presented in this paper have largely resolved the uncertainties in the geochronology of the Jurassic silicic province of Patagonia and the Antarctic Peninsula. The most reliable and consistent dataset is that obtained by U–Pb dating of volcanic zircons, using the SHRIMP. Rb–Sr whole-rock dating has proved very satisfactory for the fresh, highly welded ignimbrites of the Marifil Formation and for syn- to late-volcanic plutons. Less welded and more altered ignimbrites south of the Gastre fault zone and in the Antarctic Peninsula yield Rb–Sr ages that are $\sim$10 My too young, probably as a result of hydrothermal resetting. Ar–Ar dating of feldspars has also been suspect in the most altered rocks from the Andean outcrops and, moreover, appears to reflect initial excess ^{40}Ar in some samples of the Chon Aike Formation that have yielded apparent plateau ages older than the U–Pb zircon ages.

The new data show unambiguously that silicic volcanic activity in the region extended throughout Jurassic time, but was concentrated in three main episodes. The first of these (V1, Early Jurassic, 188–178 Ma) resulted in the eruption of a vast volume of rhyolitic ignimbrites with within-plate affinities in northeast Patagonia and the southern Antarctic Peninsula. This was coincident with the far more extensive emplacement of mafic igneous rocks in Gondwana generally associated with the Karoo mantle plume. The Middle Jurassic V2 event (172–162 Ma) represented a shift in the focus of eruption to southern Patagonia and the northern Antarctic Peninsula. The chemical characteristics suggest that magma generation occurred in continental crust with less evolved composition. The poorly welded nature of the ignimbrites suggests a lower eruptive temperature than for the highly welded ignimbrites of the Marifil Formation. The final event identified was of Late Jurassic age (V3, 157–153 Ma). It is represented by the Andean outcrops of rhyolitic ignimbrite, following a significant western shift in volcanic activity. These rocks are predominantly active-margin volcanic products and are associated with granitoids. The V3 event almost overlaps with the earliest known intrusions of the Patagonian and Antarctic Peninsula batholiths. Increased activity at this destructive margin could account for the higher degree of deformation and hydrothermal alteration in these volcanic rocks compared with those of the preceding events.

At this stage it is clear that the Jurassic volcanic province of the region is a complex polygenetic one, formed during multiple events over $\sim$35 My and probably generated by a variety of mechanisms, among which the melting of pre-existing continental crust was a dominant process. These reflect changes in the tectonic regime of Gondwana break-up, and the pattern of changing volcanism appears to be associated with the spread of heat away from the Karoo mantle plume towards the Pacific margin. However, the extended period of silicic volcanism covered the actual break-up of the region into smaller plates and their active dispersal (Fig. 9). Thus the large amount of crustal extension and thinning that must have been involved could also have been a major cause of the silicic magmatism through decompression melting. All these events preceded Early Cretaceous separation and opening of the Atlantic Ocean.

ACKNOWLEDGEMENTS

The main fieldwork on which this study is founded was carried out with invaluable assistance from Carlos Rapela, Marcelo Márquez and Patricia Sruoga (in Argentina); from Simon Abrahams, Mike Austin and BAS support staff (in Antarctica); and from Pancho Hervé (in Chile: Proyecto Fondecyt 1980741). Jorge Skarmeta and Ricardo Fuenzalida were of help in obtaining the ENAP borehole sample. The contributions of Phil Leat and Bryan Storey, both during fieldwork and in the writing of this paper, are gratefully acknowledged. Ian Millar was of great assistance during SHRIMP analyses. Helpful reviews were supplied by C. J. Hawkesworth, S. M. Kay and M. Suárez. This paper is a contribution to IGCP Project 436 (Pacific Gondwana Margin).

Note added in proof

The ages reported in this paper, and the associated westward migration of volcanism, are fully concordant

with the results and conclusions for eastern Patagonia of a new Ar–Ar study [Feraud *et al.*, *Earth and Planetary Science Letters*, **172** (1999), 83–96].

REFERENCES

Alric, V. I., Haller, M. J., Féraud, G., Bertrand, H. & Zubia, M. (1996). Cronología $^{40}Ar/^{39}Ar$ del volcanismo jurásico de la Patagonia extrandina. *XIII Congreso Geológico Argentino y III Congreso de Exploración de Hidrocarburos, Buenos Aires, Actas V.* Buenos Aires: Asociación Geológica Argentina, pp. 243–250.

Brewer, T. S., Hergt, J. M., Hawkesworth, C. J., Rex, D. & Storey, B. C. (1992). Coats Land dolerites and the generation of Antarctic continental flood basalts. In: Storey, B. C., Alabaster, T. & Pankhurst, R. J. (eds) *Magmatism and the Causes of Continental Break-up. Geological Society, London, Special Publication* **68**, 185–208.

Brewer, T. S., Rex, D., Guise, P. G. & Hawkesworth, C. J. (1996). Geochronology of Mesozoic tholeiitic magmatism in Antarctica: implications for the development of the failed Weddell Sea rift system. In: Storey, B. C., King, E. C. & Livermore, R. A. (eds) *Weddell Sea Tectonics and Gondwana Break-up. Geological Society, London, Special Publication* **108**, 45–61.

Bruce, R. M., Nelson, E. P., Weaver, S. G. & Lux, D. R. (1991). Temporal and spatial variation in the southern Patagonian batholith; constraints on magmatic arc development. In: Harmon, R. S. & Rapela, C. W. (eds) *Andean Magmatism and its Tectonic Setting. Geological Society of America, Special Paper* **265**, 1–12.

Compston, W., Williams, I. S., Kirschvink, J. L., Zhang, Z. & Ma, G. (1992). Zircon U–Pb ages from the early Cambrian time-scale. *Journal of the Geological Society, London* **149**, 171–184.

Cortés, J. M. (1981). El substrato precretácico del extremo noreste de la Provincia del Chubut. *Revista de la Asociación Geológica Argentina* **26**, 217–235.

Cox, K. G. (1992). Karoo igneous activity, and the early stages of the break-up of Gonwanaland. In: Storey, B. C., Alabaster, T. & Pankhurst, R. J. (eds) *Magmatism and the Causes of Continental Break-up. Geological Society, London, Special Publication* **68**, 137–148.

Cumming, G. L. & Richards, J. R. (1975). Ore lead isotope ratios in a continuously changing earth. *Earth and Planetary Science Letters* **28**, 155–171.

De Barrio, R. E. (1993). El volcanismo ácido jurásico en el noroeste de Santa Cruz, Argentina. *XII Congreso Geológico Argentino y II Congreso de Exploración de Hidrocarburos, Mendoza, Actas IV.* Buenos Aires: Asociación Geológica Argentina, pp. 189–198.

De Barrio, R. E., Arrondo, O., Petriella, B. & Artabe, A. (1982). Estudio geológico y paleontológico de los alrededores de la estancia Baja Pellegrini, Provincia de Santa Cruz. *Revista de la Asociación Geológica Argentina* **37**, 285–299.

De Giusto, J., Di Persia, C. A. & Pezzi, E. (1980). Nesocraton del Deseado. In: *Geología Regional Argentina, Vol. II.* Córdoba, Argentina: Academia Nacional de Ciencias, pp. 1389–1430.

Duncan, R. A., Hooper, P. R., Rehacek, J., Marsh, J. S. & Duncan, A. R. (1997). The timing and duration of the Karoo igneous event, southern Gondwana. *Journal of Geophysical Research* **102B**, 18127–18138.

Encarnación, J., Fleming, T. H., Elliot, D. H. & Eales, H. V. (1996). Synchronous emplacement of Ferrar and Karoo dolerites and the early breakup of Gondwana. *Geology* **24**, 535–538.

Fanning, C. M. & Laudon, T. S. (1997). Mesozoic volcanism and sedimentation in eastern Ellsworth Land, West Antarctica; conflicting evidence for arc migration? *Geological Society of America, Abstracts with Program* **29**, A51517.

Fanning, C. M. & Laudon, T. S. (1999). Mesozoic volcanism, plutonism and sedimentation in eastern Ellsworth Land, West Antarctica. *Eighth International Symposium of Antarctic Earth Sciences*, Wellington, New Zealand, 4–8 July 1999 (Abstract). Wellington: The Royal Society of New Zealand.

Fleming, T. H., Heimann, A., Foland, K. A. & Elliot, D. H. (1997). $^{40}Ar/^{39}Ar$ geochronology of Ferrar dolerite sills from the Transantarctic Mountains, Antarctica: implications for the age and origin of the Ferrar magmatic province. *Geological Society of America Bulletin* **109**, 533–546.

Gradstein, F. M. & Ogg, J. (1996). A Phanerozoic time scale. *Episodes* **19**, 3–5.

Gust, D. A., Biddle, K. T., Phelps, D. W. & Uliana, M. A. (1985). Associated middle to late Jurassic volcanism and extension in southern South America. *Tectonophysics* **116**, 223–253.

Heimann, A., Fleming, T. H., Elliot, D. H. & Foland, K. A. (1994). A short interval of Jurassic continental flood basalt volcanism in Antarctica as demonstrated by $^{40}Ar/^{39}Ar$ geochronology. *Earth and Planetary Science Letters* **121**, 19–41.

Hergt, J. M., Peate, D. W. & Hawkesworth, C. J. (1991). The petrogenesis of Mesozoic Gondwana low-Ti flood basalts. *Earth and Planetary Science Letters* **105**, 134–148.

Kelley, S. P. (1995). The laser microprobe Ar–Ar technique of dating. In: Potts, P. J., Bowles, F. W., Reed, S. J. B. & Cave, M. R (eds) *Microprobe Techniques in the Earth Sciences*. London: Chapman & Hall, 419 pp.

Kellogg, K. S. & Rowley, P. D. (1989). Structural geology and tectonics of the Orville Coast region, southern Antarctic Peninsula, Antarctica. *US Geological Survey Professional Paper* **1498**, 25 pp.

Leat, P. T., Scarrow, J. H. & Millar, I. L. (1995). On the Antarctic Peninsula batholith. *Geological Magazine* **132**, 399–412.

Ludwig, K. R. (1999). Isoplot/Ex 2·01: A geochronological toolkit for Microsoft Excel. *Berkeley Geochronology Center Special Publication* **1a**, 50 pp.

Malvicini, L. & Llambías, E. J. (1974). Geología y génesis del depósito de manganeso Arroyo Verde, Provincia del Chubut. *Actas del V Congreso Geológico Argentino, Villa Carlos Paz (Córdoba), Tomo II.* Buenos Aires: Asociación Geológica Argentina, pp. 185–202.

Millar, I. L., Milne, A. J. & Whitham, A. G. (1990). Implications of Sm–Nd garnet ages for the stratigraphy of northern Graham Land. *Zentralblatt für Geologie und Paläontologie, Stuttgart, Teil 1* **1/2**, 97–104.

Minor, D. R. & Mukasa, S. B. (1997). Zircon U–Pb and hornblende $^{40}Ar–^{39}Ar$ ages for the Dufek layered mafic intrusion, Antarctica: implications for the age of the Ferrar large igneous province. *Geochimica et Cosmochimica Acta* **61**, 2497–2504.

Mukasa, S. B. & Dalziel, I. W. D. (1996). Southernmost Andes and South Georgia Island, north Scotia Ridge: zircon U–Pb and muscovite $^{40}Ar/^{39}Ar$ age constraints on tectonic evolution of southwestern Gondwanaland. *Journal of South American Earth Sciences* **9**, 349–365.

Pankhurst, R. J. (1982). Rb–Sr geochronology of Graham Land, Antarctica. *Journal of the Geological Society, London* **139**, 701–711.

Pankhurst, R. J. & Rapela, C. W. (1995). Production of Jurassic rhyolite by anatexis of the lower crust of Patagonia. *Earth and Planetary Science Letters* **134**, 23–26.

Pankhurst, R. J., Sruoga, P. & Rapela, C. W. (1993). Estudio geocronológico Rb–Sr de los complejos Chon Aike y El Quemado a los 47°30′ L.S. *XII Congreso Geológico Argentino y II Congreso de Exploración de Hidrocarburos, Mendoza, Actas IV.* Buenos Aires: Asociación Geológica Argentina, pp. 171–178.

Pankhurst, R. J., Leat, P. T., Sruoga, P., Rapela, C. W., Márquez, M., Storey, B. C. & Riley, T. R. (1998). The Chon Aike silicic igneous province of Patagonia and related rocks in Antarctica: a

silicic LIP. *Journal of Volcanology and Geothermal Research* **81**, 113–136.

Parada, M. A., Palacios, C. & Lahsen, A. (1997). Jurassic extensional tectono-magmatism and associated mineralization of the El Faldeo polymetallic district, Chilean Patagonia: geochemical and isotopic evidence of crustal contribution. *Mineralium Deposita* **32**, 547–554.

Ramos, V. A. & Palma, M. A. (1981). El batolito granitico del Monte San Lorenzo—Cordillera Patagonica. *VIII Congreso Geológico Argentino, San Luis, Actas III*. Buenos Aires: Asociación Geológica Argentina, pp. 257–280.

Rapela, C. W. & Pankhurst, R. J. (1992). The granites of northern Patagonia and the Gastre Fault System in relation to the break-up of Gondwana. In: Storey, B. C., Alabaster, T. & Pankhurst, R. J. (eds) *Magmatism and the Causes of Continental Break-up. Geological Society, London, Special Publication* **68**, 209–220.

Rapela, C. W. & Pankhurst, R. J. (1993). El volcanismo ríolitico del noreste de la Patagonia: un evento meso-jurásico de corta duración y origen profundo. *XII Congreso Geológico Argentino y II Congreso de Exploración de Hidrocarburos, Mendoza, Actas IV*. Buenos Aires: Asociación Geológica Argentina, pp. 179–188.

Rapela, C. W., Pankhurst, R. J., Llambías, E. J., Labudía, C. & Artabe, A. (1996). 'Gondwana' magmatism of Patagonia: Inner Cordilleran calc-alkaline batholiths and bimodal volcanic province. *Third International Symposium on Andean Geodynamics, St Malo, France, Résumés étendus*. Paris: ORSTOM, pp. 791–794.

Renne, P. R., Swisher, C. C., Deino, A. L., Karner, D. B., Owens, T. L. & DePaolo, D. J. (1998). Intercalibration of standards, absolute ages and uncertainties in Ar–Ar dating. *Chemical Geology* **145**, 117–152.

Rex, D. C. (1976). Geochronology in relation to the stratigraphy of the Antarctic Peninsula. *Bulletin of the British Antarctic Survey* **43**, 49–58.

Riley, T. R. & Leat, P. L. (1999). Large volume silicic volcanism along the proto-Pacific margin of Gondwana: lithological and stratigraphical investigations from the Antarctic Peninsula. *Geological Magazine* **135**, 1–16.

Riley, T. R., Leat, P. T., Pankhurst, R. J. & Harris, C. (2000). Geochemistry and petrogenesis of large volume silicic volcanism (Antarctic Peninsula–South America). *Journal of Petrology* (submitted).

Rowley, P. D., Schmidt, D. L. & Williams, P. L. (1982). Mount Poster Formation, southern Antarctic Peninsula and eastern Ellsworth Land. *Antarctic Journal of the US* **17**, 38–39.

Stipanicic, P. & Bonetti, W. (1970). Posiciones estratigráficas de las principales floras jurásicas argentinas. *Ameghiniana* **7**, 57–78.

Sruoga, P. & Palma, M. A. (1984). La Formación Chon-Aike en su área clásica de afloramientos. *Actas del IX Congreso Geológico Argentino, Tomo III*, pp. 171–184.

Storey, B. C. (1995). The role of mantle plumes in continental breakup: case histories from Gondwanaland. *Nature* **377**, 301–308.

Storey, B. C., Alabaster, T., Hole, M. J., Pankhurst, R. J. & Wever, H. E. (1992). Role of subduction-plate boundary forces during the initial stages of Gondwana breakup: evidence from the proto-Pacific margin of Gondwana. In: Storey, B. C., Alabaster, T. & Pankhurst, R. J. (eds) *Magmatism and the Causes of Continental Break-up. Geological Society, London, Special Publication* **68**, 149–163.

Suárez, M. & De La Cruz, R. (1997). Edades K–Ar del grupo Ibañez en la parte oriental del Lago General Carrera (46°–47° LS), Aysén, Chile. *8° Congreso Geológico Chileno, Antofagasta, Actas 2*. Antofagasta: Universidad Catolica del Norte, pp. 1548–1551.

Tangeman, J. A., Mukasa, S. B. & Grunow, A. M. (1996). Zircon U–Pb geochronology of plutonic rocks from the Antarctic Peninsula: confirmation of the presence of unexposed Palaeozoic crust. *Tectonics* **15**, 1309–1324.

Thomson, M. R. A. & Pankhurst, R. J. (1983). Age of post-Gondwanian calc-alkaline volcanism in the Antarctic Peninsula region. In: Oliver, R. L., James, P. R. & Jago, J. B. (eds) *Antarctic Earth Science*. Canberra: Australian Academy of Science; Cambridge: Cambridge University Press, pp. 328–333.

Wever, H. E. & Storey, B. C. (1992). Bimodal magmatism in northeast Palmer Land, Antarctic Peninsula: geochemical evidence for a Jurassic ensialic back-arc basin. *Tectonophysics* **205**, 239–260.